MASTER IN BIOLOGY OF ORGANISMS AND ECOLOGY

The evolutionary potential of DNA methylation in the gonads of two populations of the mangrove rivulus (Kryptolebias marmoratus) and its developmental reprogramming

Alexandrescu, Gauthier

Award date:
2024

Awarding institution:
University of Namur
Université Catholique de Louvain

Université catholique de Louvain
École de biologie

Université de Namur
Département de biologie

The evolutionary potential of DNA methylation in the gonads of two populations of the mangrove rivulus (*Kryptolebias marmoratus*) and its developmental reprogramming

Alexandrescu Gauthier

Master's thesis presented to obtain the degree of
Master in Organismal Biology and Ecology

Promoter: Pr. Frédéric Silvestre
Supervisor: Justine Bélik

Academic year of 2023 - 2024

Preamble

This master's thesis is the result of a one-year work in the Laboratory of Evolutionary and Adaptive Physiology at the University of Namur. This work is written as a scientific article format and is submitted in partial fulfillment of the requirements for the degree of Master in Biological Sciences, specifically oriented towards Organismal Biology and Ecology. Therefore, this project follows the traditional scientific article format, that is starting with an introduction, then explaining the material and methods which were used, followed by showing the results obtained, discussing these results with the scientific literature, and finally stipulate the conclusion of this work. References used throughout this work, data and code availability, as well as supplementary information and annexes can be found at the end of this paper. The introduction to scientific research (bibliographical introduction of the subject submitted in June 2023) is also attached at the end.

Acknowledgements

This master's thesis has been for me the first real taste of a researcher's life. It has honestly been a great opportunity for which I am fortunate to take part throughout this master program. I have been able to design my own project, all the way from choosing a pleasing subject, asking the research questions, elaborating the protocols with modern techniques and technologies, practicing laboratory work and as such gaining practical experience, analyzing the data and subsequent results, and finally writing this master's thesis under a scientific article format, forming myself for scientific communication.

Firstly, I would like to thank my promoter, Pr. Frédéric Silvestre, for giving me the freedom to design my project, research questions, laboratory work, and scientific reasoning, always with kindness and advanced reflection towards achieving the fixed goals. Thank you for everything you have taught me.

I also would like to express my gratitude to Jérôme Lambert, the laboratory technician who assisted me from the beginning until the end of this work. You have such an impressive knowledge of the laboratory techniques. I have learned a lot from you, with such high-quality information. We have had a few very funny moments together, likewise some doubtful and intense times, but it is all part of science. A huge thank you for you Jérôme.

Thank you Justine and Ivan for assisting me during this master's thesis and helping me making my way in the laboratory. I had a great time sharing knowledge with you, either related to biology or not.

Finally, I would mostly like to thank my parents and my sister for their daily support throughout this experience. I am forever thankful for your transmitted motivation and love. Having you by my side during this master's thesis was a key component for making it an accomplishment.

I am grateful for this whole experience, from the highs and lows, the laughs and doubts, the lessons, the setbacks and comebacks, because it made this master's thesis the way it is, presented here. Hard work pays off, sooner or later, but it always does.

Abstract

The field of epigenetics is a fascinating research area focusing on the regulation of DNA sequence. More specifically, DNA methylation is an epigenetic mechanism vastly studied in a myriad of organisms allowing to link gene expression with phenotypic plasticity. The mangrove rivulus (*Kryptolebias marmoratus*) is an ideal model organism for studying the epigenetic roles in the regulation and expression of phenotypic traits, as it is one of only two vertebrates capable of self-fertilization. This ultimately allows to specifically scope epigenetic mechanisms while drastically reducing genetic variation between individuals. This work therefore aims to study the evolutionary potential of DNA methylation in two populations of the mangrove rivulus exhibiting a differential genetic background. A first approach studies the methylome in the gonads using Reduced-Representation Bisulfite Sequencing (RRBS), targeting CpG-rich DNA regions of the genome where cytosine methylation is known to be abundant in vertebrates. A second approach targets gene-specific methylation of key epigenetic actors, namely *DNMT3a* (DNA Methyl-Transferase 3a), *MeCP2* (Methyl CpG binding Protein 2), and *NIPBL* (Nipped-B-like protein B) in three developmental stages of *K. marmoratus*, using bisulfite pyrosequencing. RRBS study on the gonads of hermaphroditic fish shows a close methylation pattern within cytosine distribution in both populations. The differential methylation of CpGs (DMCs) and of regions (DMRs) showed that 1.230% of the CpGs and 4.236% of the regions are significantly differentially methylated between the two populations on the reverse strand of DNA. Pyrosequencing analysis on the other hand reveals interestingly variable methylation between the targeted sequences. Notably, the second intron of *DNMT3a* and the promoter region of *NIPBL* demonstrated a significant effect of the developmental stages on the methylation status of the studied sequences, showing progressive demethylation and increasing methylation, respectively, while progressing through embryogenesis. Evolutionary potentials are discussed following the DNA methylation patterns discovered throughout this research. This work promotes further investigation on the contribution of DNA methylation towards phenotypic plasticity using cutting-edge technologies, especially with the mangrove rivulus which has unique natural characteristics permitting to decipher relevant epigenetic questions.

Keywords: epigenetics, mangrove rivulus, gonads, DNA methylation, reprogramming, RRBS, pyrosequencing.

1 | Introduction

The recent advances in sequencing technologies as well as the development of techniques profiling epigenetic marks and chromatin accessibility using reagents applicable in any species have rocketed epigenomic studies in multiple animal species **(Sadler, 2023)**. Epigenetics are mitotically and/or meiotically heritable changes in gene expression that cannot be explained by changes in the gene sequence, therefore epigenetic variation does not alter the underlying nucleotide sequence **(Russo *et al.*, 1996; Youngson & Whitelaw, 2008; Lamka *et al.*, 2022)**. Such changes are mainly represented by DNA methylation, histone modifications and small RNA regulation, which are implied in processes such as cellular differentiation and development, behaviors, metabolism, morphology, and physiological phenotypes for example, by affecting gene expression and protein synthesis **(Nicoglou & Merlin, 2017; Perez & Lehner, 2019; Lamka *et al.*, 2022)**.

Growing recent evidence suggests that epigenetic variation, like genetic variation, may also contribute to shape phenotypic responses **(Hu & Barrett, 2017)**. Epigenetic mechanisms indeed affect ecologically important traits even in the absence of genetic variation **(Kilvitis *et al.*, 2014)**. These mechanisms manage gene expression and their products in a real-time perspective, allowing a single genome to display different phenotypes without any genetic sequence modification **(Angers *et al.*, 2010; Verhoeven & Preite, 2014)**. Because epigenetic marks can be directly affected by the environment, epigenetic variation can play a primary role in an organism's response to environmental fluctuations, procuring an ideal mean for directional and fast adaptation to changing or novel conditions **(Daxinger & Whitelaw, 2010; Vogt, 2022; Chapelle & Silvestre, 2022)**. Therefore, epigenetics could be seen as the "missing link" between environmental and phenotypic variations **(Herrel *et al.*, 2020)**. In addition to being another source of heritable phenotypic variation, epigenetic variation can precede genetic adaptation *via* genetic accommodation (*i.e.*, quantitative genetic change in the frequency of genes affecting the regulation or form of a new trait **(West-Eberhard, 2003, 2005)**), thus reversing the common model of evolution from a genotype-to-phenotype to a phenotype-to-genotype circuit **(West-Eberhard, 1986; Jablonka & Lamb, 1989)**, possibly driving rapid evolution **(Skinner, 2015)**. When compared with genetic variation, epigenetic variation is more prompt to have higher spontaneous rates of mutation as well as enhanced sensitivity reaction to environmental stimuli, perhaps providing the raw material for phenotypic selection when genetic variation is limited **(Drake *et al.*, 1998; Ossowski *et al.*, 2010; Becker *et al.*, 2011; Schmitz *et al.*, 2011; Zhang *et al.*, 2013)**. Hence, an evolutionary potential of epigenetic variation can be proposed due to its autonomy from genetic variation, in addition to its transgenerational stability (inherited *via* non-mendelian processes) **(Hu & Barrett, 2017; Chapelle & Silvestre, 2022)**. Consequently, the extended theory of evolution ultimately includes epigenetic variation as an evolutionary mechanism in natural populations **(Schrey *et al.*, 2012; Laland *et al.*, 2015; Chapelle & Silvestre, 2022)**.

DNA methylation, the most broadly characterized epigenetic mechanism in both plants and animals **(Ambrosi *et al.*, 2017; De Mendoza *et al.*, 2020; Peixoto *et al.*, 2020),** is crucial for vertebrate development and

procures a plastic but still stable information in addition to the DNA code **(Ortega-Recalde & Hore, 2019)**. This mechanism occurs across all taxa of life and is primarily referring to the transfer of a methyl group to position 5 of cytosine residues, forming 5-methylcytosine (5mC) in prokaryotes and eukaryotes **(Zemach *et al.*, 2010; Ambrosi *et al.*, 2017)**. Specifically, in vertebrates, the extent and the pattern of DNA methylation are well conserved throughout species as it takes place nearly across the whole genome, with 70-80% of cytosines included in CpG dinucleotides being methylated **(Feng *et al.*, 2010)**.

An obstacle that must be overcome to study the role of epigenetic variation in evolution is that DNA sequence differences among individuals can rarely be excluded to explain heritability of phenotypes **(Fellous *et al.*, 2018)**. Thus, a clear understanding of the role of epigenetic variation in evolution can better be achieved in individuals that are genetically identical while displaying a range of heritable phenotypes in nature **(Heard & Martienssen, 2014)**. The mangrove rivulus (*Kryptolebias marmoratus*), natively found in mangrove ecosystems, and its sister species *Kryptolebias hermaphroditus*, are the only known vertebrates able to self-fertilize **(Harrington, 1961; Tatarenkov *et al.*, 2009; Costa, 2011)**. This kind of sexual reproduction is called selfing, and in long term it results in individuals with completely homozygous genotypes **(Earley *et al.*, 2012; Tatarenkov *et al.*, 2012)**. The selfing rate is variable depending on the ratio of males (low proportion, mostly fewer than 5%, there are primary and secondary males) in the population, however there are no females. This is a natural demonstration of a rare androdioecious mixed reproductive system, by alternative selfing and outcrossing with males **(Scott Taylor, 2012; Ellison *et al.*, 2015)**. Therefore, as examples, genetically diverse individuals can mainly be found in populations from Belize composed of 41.8% of males, whereas numerous isogenic ("clonal") lineages can be found in populations from Florida encompassing 0.4% of males **(Tatarenkov *et al.*, 2015; Chapelle, 2023)**. The methylome of *K. marmoratus* exhibits conserved vertebrate characteristics, because like mammals and other teleost fish, its genome has high levels of DNA methylation genome-wide in the CpG context **(Voisin *et al.*, 2022; Chapelle, 2023)**.

It is increasingly apparent that animals not only transmit DNA but also a variety of other informational molecules, such as proteins, RNA, and metabolites, to their descendants *via* gametes **(Perez & Lehner, 2019)**. This information can be altered following change in the physiological and environmental conditions of previous generations, however a current question is whether epigenetic mechanisms can procure a heritable and potentially adaptive memory of anterior environmental exposure **(Heard & Martienssen, 2014)**. Generally, epigenetic marks are cleared out and re-established at each generation, nonetheless at certain loci in the genome, this resetting isn't complete, which is referred to as transgenerational epigenetic inheritance (TEI) **(Daxinger & Whitelaw, 2010)**. To be inherited, epimutations must overcome DNA methylation reprogramming, which happens twice: once in the germline and once in the early embryo **(Grossniklaus *et al.*, 2013; Fellous *et al.*, 2018)**. Reprogramming is an erasure of epigenetic marks required for correct development of the embryo and an establishment of DNA methylation patterns in the new individual **(Monk *et al.*, 1987)**. After fertilization, a specific pattern of CpG DNA methylation reprogramming is characterized

for *K. marmoratus* during embryogenesis, as it occurs particularly later, lasts longer and is more dramatic than reported at similar embryonic stages of other studied vertebrates (notably compared to zebrafish) **(Fellous *et al.*, 2018)**.

This work aims to study the contribution of DNA methylation to the evolution and adaptation of the mangrove rivulus by examining the DNA methylation pattern variation within and between on the one hand wild *K. marmoratus* populations and, on the other hand, fish reared under standardized laboratory conditions. The mangrove rivulus brings the exceptional opportunity to work on both genetically diverse and clonal populations due to its natural characteristics, allowing to investigate phenotypic plasticity and the regulation of development and reproduction by epigenetic variance **(Fellous *et al.*, 2018, 2019)**. This eventually permits for the comparison of populations covering a range of genetic diversity. Two populations of *K. marmoratus* are specifically targeted in this study: the first population comes from Emerson Point Preserve (EPP; Florida), which is characterized by a low genetic diversity between the individuals, thus more isogenic fish are expected. The second population comes from Twin Cayes (TC; Belize), where the fish exhibit a higher genetic variability between them, hence less isogenic fish are awaited **(Tatarenkov *et al.*, 2015; Chapelle, 2023)**. Because the mangrove rivulus is a vertebrate species, CpG dinucleotides will be the target of this work's DNA methylation analyses. To investigate the balance between epigenetic and genetic variations in these two populations of *K. marmoratus* and to add knowledge on how these variations allow this fish to live in its fluctuating wild environment, the first part of this study will assess the level of DNA methylation in the gonads of hermaphroditic fish among EPP and TC populations. The gonads are of crucial significance for studying an evolutionary question, since a transgenerational aspect of epigenetic marks would be needed to correctly talk about evolution **(Fellous *et al.*, 2018)**. By choosing Reduced-Representation Bisulfite Sequencing (RRBS) as the optimal technique for this research, differentially methylated CpGs (DMCs) and regions (DMRs) are searched using a bisulfite conversion of DNA with an enrichment for CpG-rich regions. To reinforce the results from the above research, a second study focuses on the epigenetic reprogramming of three distinct stages of the embryonic development of this fish, namely the gastrula stage, the Otic-Lens formation (OL) and the 27th stage. The epigenetic reprogramming will help to understand if DNA methylation marks at precise stages of *K. marmoratus* development are expressed or not, effectively giving insights on the epigenetic roles, even at the basic stages of life. Bisulfite pyrosequencing was thus performed for studying the reprogramming event in the three embryonic stages as it permits to tackle gene-specific methylation of three genes which were previously studied for the mangrove rivulus by **Chapelle (2023)** for their DNA methylation relevance: *DNMT3a* (DNA Methyl-Transferase 3a), *MeCP2* (Methyl CpG binding Protein 2), and *NIPBL* (Nipped-B-like protein B). The first studied gene is *DNMT3a*, as it codes for the *de novo* methylation enzyme DNMT3a, which explains the acquisition of DNA methylation on both strands of DNA, independently of DNA replication **(Okano *et al.*, 1999; Goll & Bestor, 2005; Ambrosi *et al.*, 2017)**. The second studied gene is *MeCP2*, as it codes for the methyl-DNA-binding domain (MBD) protein MeCP2 recruited to methylated CpG, where it regulates transcription and chromatin organization **(Kriaucionis &**

Bird, 2003; Song *et al.*, 2014). The last gene studied is *NIPBL*, coding for the protein NIPBL, which contributes to the regulation of genome-controlled gene expression *via* the action of cohesin in chromosome structure **(Gao *et al.*, 2019)**. The interaction of NIPBL with chromatin factors, the transcriptional machinery and replication proteins, intervene critically and regulatorily in cohesin distribution, in the loading on chromatin, in gene expression and in transcriptional signaling **(Alonso-Gil & Losada, 2023)**. Together, these two research permit to examine DNA methylation patterns between two populations of *K. marmoratus* exhibiting a distinct genetic diversity, firstly by approaching a restricted portion of the genome in a tissue never studied this way before for this fish, but also by studying gene-level regulation of key epigenetic actors.

2 | Material and methods

2.1 | Mangrove rivulus gonad origins

The gonads analyzed in this study come from 82 adult hermaphrodite mangrove rivulus captured by Valentine Chapelle, Frédéric Silvestre, and Ryan Earley, during fieldwork in 2019. Two populations are specifically targeted, one from South Florida (Emerson Point Preserve (EPP), Palmetto, Florida, USA; N27°31'56.8", W82°37'46.4"), and the second one from Belize (Twin Cayes (TC), Papa Gabriel, Belize; N16°83'11.8'', W88°09'94.0"). After dissection, the gonads were kept in RNA Later Stabilization Solution (Invitrogen) and brought back to Belgium and stored in the Laboratory of Evolutionary and Adaptive Physiology (LEAP, University of Namur, Belgium), at -80°C until DNA extraction.

2.2 | Fish rearing

Adult rivulus from EPP and TC isogenic lineages were reared for the collection of their eggs under laboratory conditions. Fish were kept individually in 12 ± 1 parts per thousand (ppt) saltwater reconstituted by mixing marine salts (Instant Ocean® Sea Salt) with demineralized water, in a 500 mL plastic aquarium in controlled conditions, namely at 25°C, 12:12 light:dark photoperiod, and fed everyday *ad libitum* with living *Artemia salina* nauplii (ArFiDel sprl). Small pieces of cotton were added inside the tanks to offer a shelter (animal wellbeing) and an oviposition substrate. During the eggs' collection period, those fish received daily additional *ad libitum* bloodworms (Ocean Nutrition™) after the egg collection was achieved. More information on the renewal of fish and artemia waters is available in **Supplementary information 1**.

2.3 | Egg collection

Eggs from EPP and TC populations were collected every day from the beginning of July until mid-August (6 weeks period). Importantly, TC fish from which eggs were collected were brought back to Belgium as eggs from a fieldwork in Belize in late-spring 2023. The analysis of developmental stages was led by microscopic observation of morphological and mobility criteria following the descriptions of **Mourabit *et al.* (2011)**. The stages selected were the gastrula stage (stages 10 to 14, 15-25.5 hpf (hours post-fecundation)), the otic vesicle formation and the lens formation (stages 18 and 19, respectively, 43.5-53 hpf), redefined in this work as the Otic-Lens formation (OL) stage, and the 27th stage of development (stages 27a and 27b, representing increased

pigmentation and body movement, 105-120 hpf) **(Annex 1)**. The collected eggs were placed individually or by group depending on the number of eggs sampled for a single fish when collecting, in a plastic 24-wells plate (Greiner Bio-One, Cellstar®), with 2 mL of 12 ± 1 ppt of saltwater. The plates containing the eggs were placed in an incubator at 25°C with a 12:12 light:dark photoperiod **(Figure S1)**. Saltwater was changed once a week, until a matching embryonic stage was found. Eggs at a desired stage were placed in a 96-wells plate under -80°C. Eggs were pooled by stage to obtain a minimum of 35 ng of DNA per mL. Three replicates of a pool were created per population, with the exceptions of the gastrula and OL stages for TC population which collated only 1 pool of 15 eggs and 1 pool of 10 eggs respectively, due to a standstill egg laying period. Therefore, 14 pools were created in total: 3 pools of 7 eggs for the 27th stage (x2 for EPP and TC populations), 3 pools of 14 eggs for the OL stage (achieved for EPP, not for TC), and 3 pools of 20 eggs for the gastrula stage (achieved for EPP, not for TC).

2.4 | DNA extraction

Genomic DNA from the gonads of 82 wild mangrove rivulus (42 gonads from EPP population and 40 gonads from TC population) and from the embryonic stages collected was extracted using the NucleoSpin® Tissue XS kit (Macherey-Nagel, 740901.250, Düren, Germany) following the manufacturer's instructions. This extraction begins with a digestion by proteinase K which is incubated with the tissue for 18 hours (overnight, for the gonads) or approximately 2 hours for the eggs at 56°C. The obtained lysate was subsequently transferred into columns and washed several times to eluate 20 µL of gDNA for the gonads, and 22 µL of gDNA for the eggs. This final elution is then stored at -20°C for further analyses, respectively RRBS analysis for the gonads and gene-specific DNA methylation analysis by pyrosequencing for the developmental stages.

2.5 | DNA quality and quantity assessment

All the 82 gDNA extractions of the gonads were tested for DNA quality and quantity. The first test was realized by spectrophotometry *via* Nanodrop (NanoDrop 2000c spectrophotometer, Thermo Scientific) aiming to estimate the DNA and RNA combined concentration in ng/µL as well as the 260/280 nm and 260/230 nm ratios in the extractions. Then a Qubit™ fluorometer (Invitrogen™) Broad-Range test was effectuated (with 1 µL of sample input) to measure the concentration of DNA in each sample in µg/mL. Finally, the evaluation of DNA integrity was performed with two 1% agarose gel electrophoreses. Those gels were testing a few samples from the following categories: 1) samples showing good Nanodrop estimation of concentrations, good ratios (260/280 and 260/230 ratios around the value of 2), and acceptable Qubit concentrations (more than 20 µg/mL); 2) diluted samples with Ambion™ Nuclease-Free Water (Invitrogen, Thermo Fisher Scientific); and 3) samples showing low Nanodrop concentrations and ratios as well as low DNA concentrations measured from Qubit. DNA samples were then stored at -20°C for the ensuing RRBS analysis. For each population, 24 samples encompassing the greatest DNA quality were selected for further library preparation. Concerning the eggs, only a Qubit Broad-Range test was performed to have an idea of

DNA concentration in each sample and limit the utilization of sample volume since eggs have relatively lower amounts of DNA extracted.

2.6 | RRBS library preparation and sequencing

RRBS relies on a bisulfite treatment of gDNA, where unmethylated cytosines are converted into uraciles (therefore into thymines after PCR amplification) whereas methylated cytosines remain the same. The library was prepared based on 24 samples of each population selected out of the 82 total extractions. Library preparation was made using the Diagenode Premium RRBS Kit V2, Cat. No. C02030036 (24 rxns, 2x) (Diagenode, Belgium), following the manufacturer's instructions, with 100 ng of purified DNA as starting material. Each gonad identification was renewed for the library, which was given according to the initial sample concentration of DNA (Qubit result), therefore permitting a randomization of samples' identification and population while using the kit. This kit allows for RRBS on Illumina® platforms (Illumina®, Inc., USA), and encounters an enzymatic digestion (MspI enzyme, which is insensitive to the methylation status of the recognition site, CCGG), the library preparation, a size selection step with Agencourt® AMPure® XP Beads (Beckman Coulter, A63880), a quantification step *via* qPCR (StepOnePlus (Real-Time PCR System), Applied Biosystems), a sample pooling step (reducing the number of samples based on their Ct values), followed by a bisulfite conversion encountering the resuspension of the library with 22 µL of bisulfite elution buffer, and finally the library amplification (also containing a purification with AMPure® XP Beads). From then on, the library was sent to the GIGA platform, at the University of Liège, for further analyses and sequencing. The library was once again quantified by qPCR and quality control of the samples (integrity and size of DNA) was performed on this last step with a QIAxcel Advanced Instrument (Qiagen), ultimately leading to next-generation sequencing with an Illumina NovaSeq6000 S4 V1.5 machine (300 cycles) as paired-end sequencing, 150bp reads, with a minimum sequencing depth of ~20 million reads per sample.

2.7 | Gene-specific DNA methylation using pyrosequencing

Pyrosequencing was preceded by a bisulfite treatment. This treatment was performed on samples' gDNA with EZ DNA Methylation kit from Zymo Research (ref: D5002). All the 22 µL of elution volume from DNA extraction of the eggs was used given the low amount of DNA collected. The manufacturer's protocol was followed except for the elution step: two elutions of 10 µL using M-Elution Buffer instead of a single 10 µL elution were performed to double the elution volume for the subsequent analysis.

PCR amplification was firstly carried out using PyroMark PCR Kit from Qiagen (ref: 978703) in 25 µL reaction volumes containing 1 µL of sample DNA, 6 µL of nuclease-free water, 12.5 µL of 2x PyroMark PCR Master Mix, 1 µL of $MgCl_2$, 2.5 µL of 10x CoralLoad Concentrate (loading dye), and 2 µL of forward and reverse primers. The manufacturer's instructions were followed for PCR conditions.

The three genes tackled here were already studied by **Chapelle (2023)**, who designed the primers for several sequences of these targeted genes **(Annexes 2 & 3)**. These primers were analyzed for biological and technical

(gel electrophoreses **(Annex 4)**) validations of relevance for this study, eventually leading to the selection of all these sequences for this work. In the LEAP laboratory, the first step towards designing primers for pyrosequencing implies the use of the PyroMark Assay Design SW 2.0 software (Qiagen). This software permits to design forward and reverse primers for PCR and sequencing primers for pyrosequencing from the selected DNA sequences of the genes of interest. The website MethPrimer **(Li & Dahiya, 2002)** is used to spot CpG islands across each sequence (promoter region, exons, and introns). Ulteriorly, Match^{TM} **(Kel *et al.*, 2003)** is used to highlight smaller sequences containing binding sites of transcription factors (TF) whose biological roles are relevant to the study. Sequences of about 150bp are selected, containing CpG islands as well as TF binding sites in promoters, exons, and introns. Pyrosequencing was performed using the PyroMark Q24 platform and its associated WorkStation with PyroMark Q24 Advanced Reagents (Qiagen) following the manufacturer's instructions, with a 15 µL input of PCR product. The resulting pyrograms were thereafter manually interpreted and evaluated to quantify and visualize the methylation of cytosines in the specific region studied, utilizing the PyroMark Q24 Advanced software.

2.8 | Data analysis: biostatistics and bioinformatics

2.8.1 | RRBS analysis of DNA methylation from the gonads of EPP and TC populations

Firstly, the raw paired-end data obtained from Illumina sequencing was demultiplexed to get an individual fastq file per sample tested, using cutadapt (v3.5) **(Martin, 2011)**. Only the reverse strand of DNA was successfully demultiplexed, therefore, with the short remaining allotted time, subsequent analyses were performed uniquely on this strand. Trim Galore (v0.6.6) **(Krueger, 2012)**, which is using cutadapt, was then run to trim the adaptors, remove low quality nucleotides (< 20 of Phred score), and to remove the end-repaired cytosines at the extremity of DNA sequences. Trim Galore also wraps FastQC (v0.11.9) **(Andrews, 2010)**, which allows for the assessment of quality of the sequencing data. Default parameters were used, in addition to these specific options: --rrbs, --non_directional, --quality 28, --illumina, --stringency 2, and --length40. Trimmed reads were aligned with the bisulfite mapping tool Bismark (v0.24.0) **(Krueger & Andrews, 2011)** to the latest *K. marmoratus* genome assembly (RefSeq assembly accession: GCF_001649575.2 (2020)) with a few adjusted parameters (--score_min L, 0, -0.6). Lastly, Samtools **(Li *et al.*, 2009)** was used to sort by chromosome and read position the .bam files from Bismark and to index them. Successive data analysis occurs in the statistical software RStudio (v4.3.2) using the package methylKit (v1.28.0) **(Akalin *et al.*, 2012)**. This package is used to analyze differentially methylated CpGs (DMCs) and regions (DMRs, using tiles (regions) of CpGs). Analyses were eventually made on 25 gonad samples, 16 from EPP and 9 from TC. FilterByCoverage function was firstly used to filter and discard cytosines that had a read coverage lower than 10 and having more than the 99.9th percentile coverage in each sample. The coefficient of variation (CV) for each CpG and tile in EPP and TC populations was calculated by dividing the standard deviation by the mean methylation, altogether multiplied by 100. CV is an indicator of the total variability of methylation between the samples. DMC analysis was performed by applying a logistic regression with correction for overdispersion, using a Chi-square test. Significance was determined for every comparison using a minimum

percent methylation difference between the two populations of 10% and a q-value (adjustment of p-value for multiple test correction) ≤ 0.01. DMR analysis followed the same workflow with a minimum coverage of 3%, using the tiling window approach with a 300bp window size and 300bp step size to determine DMRs between the two populations, because statistically, the number of pieces of information available for a single-CpG site is lower than for a region, hence a comparison of a single site is less sturdy than that of a region **(Chatterjee *et al.*, 2017)**.

2.8.2 | Pyrosequencing analysis of DNA methylation in specific genes

All statistical analyses for studying the output data from pyrosequencing were performed in RStudio (v.4.3.2). These analyses were done on a single-sequence level. Firstly, a Shapiro-Wilk normality test was performed for checking the normal distribution of the obtained raw data, complemented by a normal Q-Q plot. The homogeneity of variances was tested with either a Bartlett's (parametric) or Levene's (non-parametric) test following the normal distribution of the data, accompanied by visual interpretations on the associated plot. Then, either a one-way ANOVA (parametric) or a Kruskal-Wallis test (non-parametric) was performed, followed by a post-hoc test (Tukey for multiple comparisons of means or Dunn's test for pairwise multiple comparisons of mean ranks, respectively). Additionally, a Generalized Linear Model (GLM) quasibinomial was also realized, testing a model for effect prediction of the developmental stages on the mean ratio (proportion) of methylation. For all statistical analyses, the p-value was fixed to a threshold of 0.05. Statistical results ≤ 0.05 were defined as significant.

3 | Results

3.1 | Cytosine distribution and related methylation on the reverse strand of DNA in the gonads

Bismark analysis procures reports for each sample, describing the number of cytosines either methylated or not in CpG, CHG, CHH and unknown (CN or CHN) contexts (H represents either A, T, or C nucleotides; N represents an unknown nucleotide), as well as the associated methylation percentages. The following figure **(Figure 1)** firstly demonstrates global cytosine distribution (number of methylated and unmethylated cytosines) in the diverse contexts, regrouping EPP and TC populations. Cytosines are mainly distributed within CHH context in both populations. Methylation percentages in each context within a particular population are then shown, where CpG context is the most methylated in both populations.

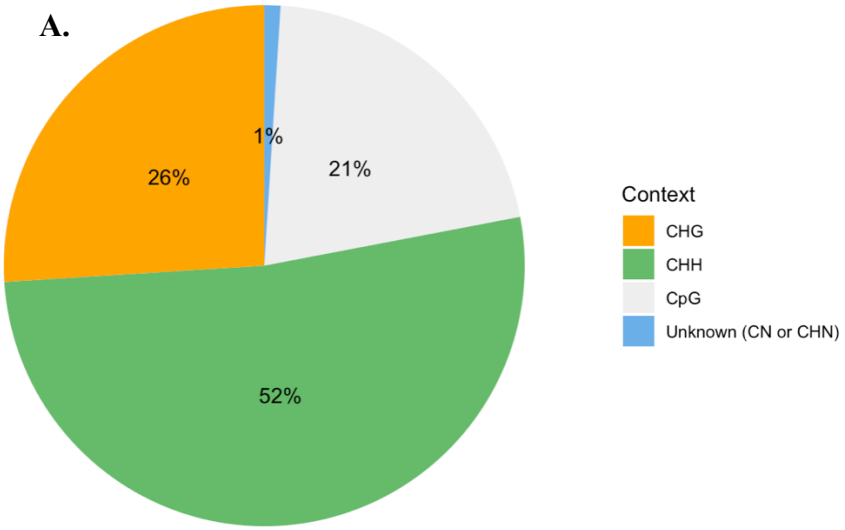
A.
26%
1%
21%
52%
Context
CHG
CHH
CpG
Unknown (CN or CHN)

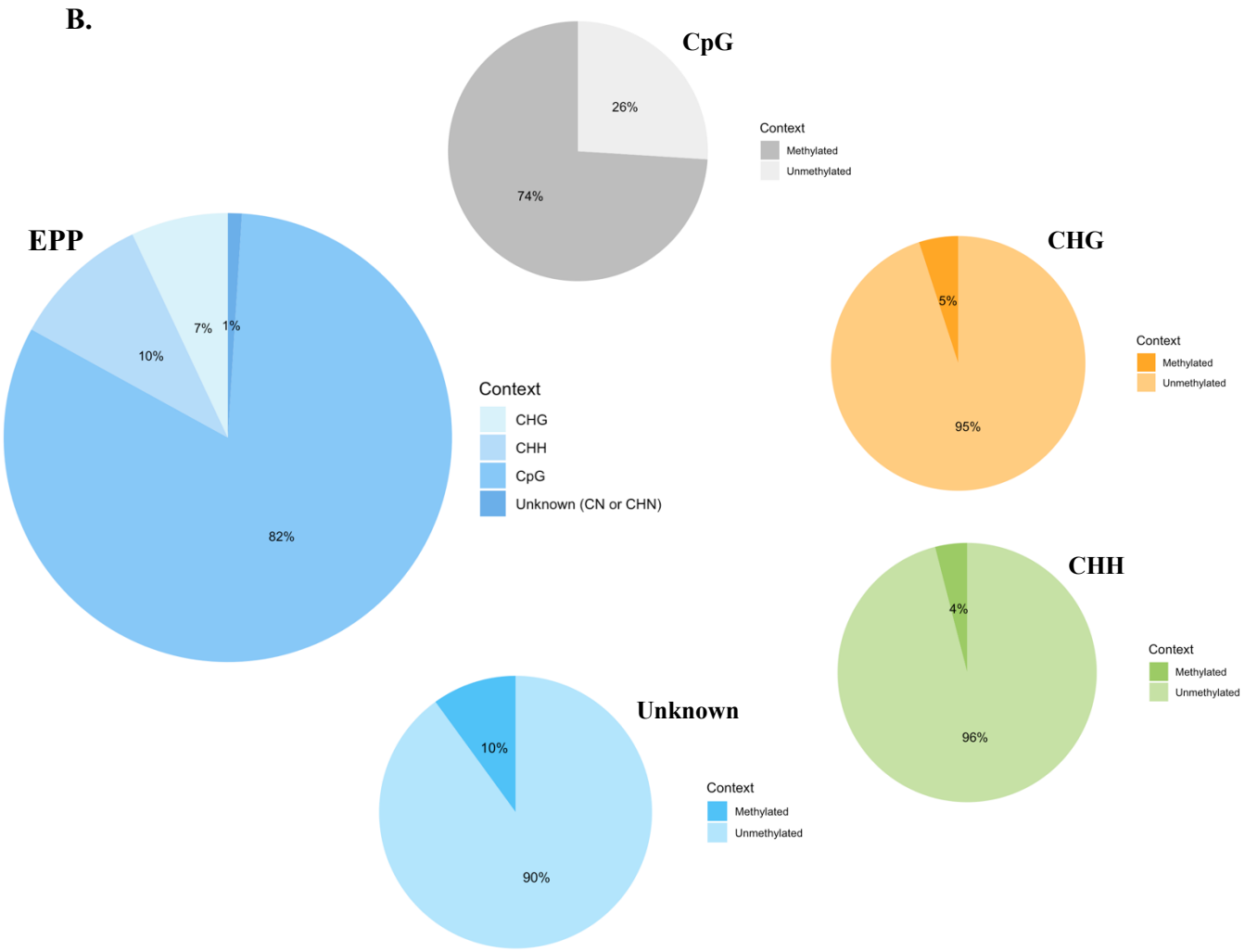
B.
CpG
26%
74%
Context
Methylated
Unmethylated
EPP
7%
1%
10%
82%
Context
CHG
CHH
CpG
Unknown (CN or CHN)
CHG
5%
95%
Context
Methylated
Unmethylated
CHH
4%
96%
Context
Methylated
Unmethylated
Unknown
10%
90%
Context
Methylated
Unmethylated

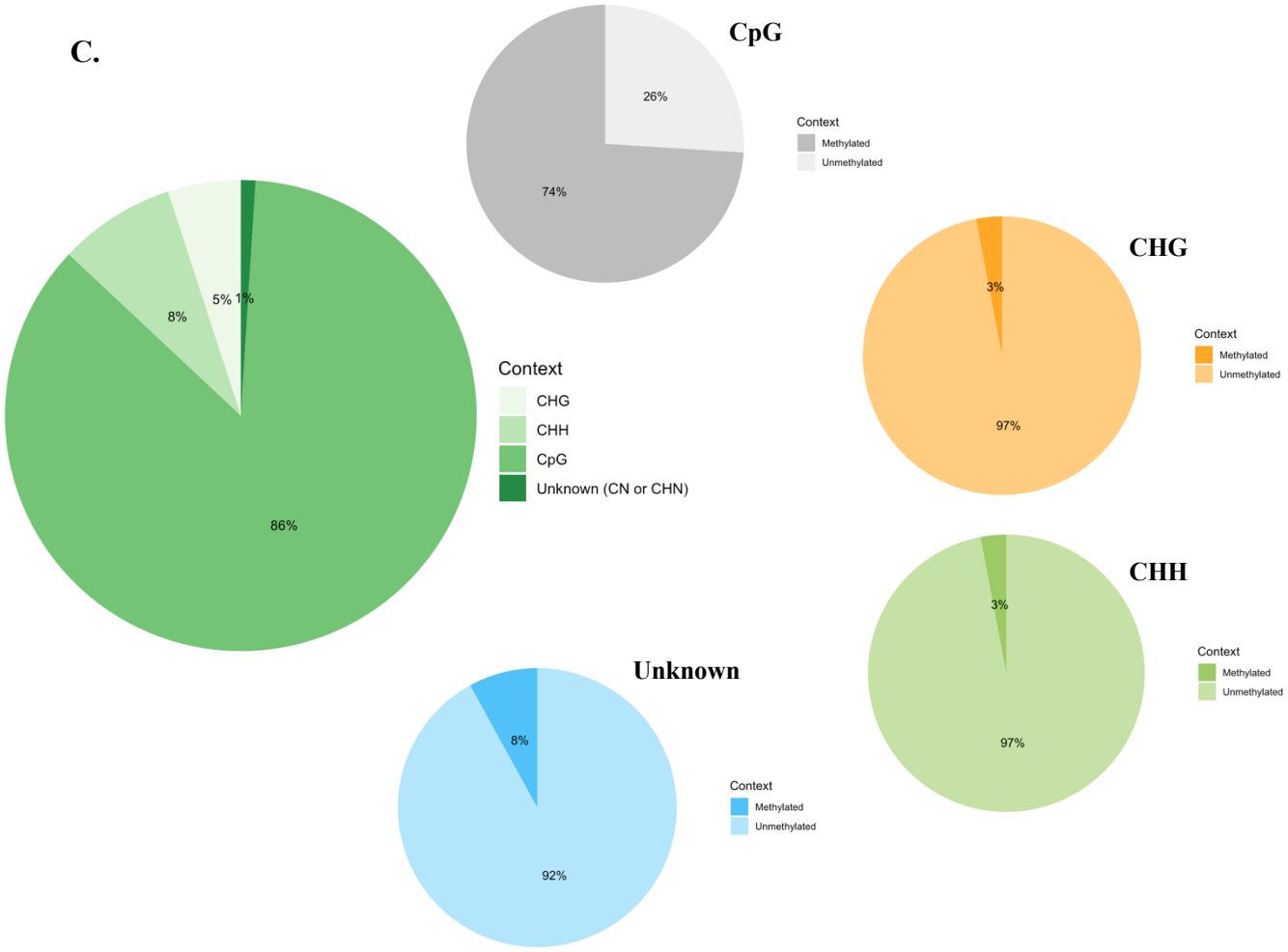

Figure 1: Details of gonad cytosine distribution and methylation on the reverse strand of DNA for EPP and TC populations of the mangrove rivulus. Cytosine distribution regroups CpG, CHG, CHH, or unknown (CN or CHN) contexts. A. Global distribution of cytosines in the four contexts, regrouping both EPP and TC populations (N= 25). In total, there are 225 775 071 cytosines distributed in the CpG context, 285 427 500 in the CHG context, 576 608 122 in the CHH context and 1 719 735 in the unknown context (regrouping EPP and TC samples). B. Cytosine methylation percentages in the four contexts for EPP population (N= 16). There are in total 64 772 835 cytosines methylated in the CpG context, 5 293 079 in CHG context, 7 683 330 in CHH context, and 59 695 in the unknown context. C. Cytosine methylation percentages in the four contexts for TC population (N= 9). There are in total 103 180 420 cytosines methylated in the CpG context, 5 481 337 in CHG context, 9 340 265 in CHH context, and 84 102 in the unknown context. The specific cytosine methylation and non-methylation percentages are described for each population in reduced format. H= A, T or C; N= unknown nucleotide.

3.2 | RRBS study of differentially methylated CpGs

The calculation of the coefficient of variation of methylation for each CpG in EPP and in TC populations revealed a mean CV of 32.13% for EPP and 5.62% for TC. The mean of differential methylation is -16.34% in EPP compared to TC (mean q-value= 1.127e-03), with a maximum of differential methylation of 100.00% (hypermethylated) and a minimum of -100.00% (hypomethylated) at the CpG level in EPP compared to TC. In a total of 71 540 differentially methylated CpGs between the populations, 879 are defined as significantly differentially methylated with the defined thresholds, that is a minimum percent methylation difference between the two populations of 10% and a q-value ≤ 0.01. This means that 1.230% of the CpGs are significantly differentially methylated between EPP and TC populations on the reverse strand of DNA for the

gonad tissue. The mean of hypermethylated DMCs is 26.99% (q-value= 1.309e-03), and the mean of hypomethylated DMCs is -35.34% (q-value= 1.047e-03) between the two populations, using the same threshold parameters as above.

3.3 | RRBS study of differentially methylated regions

The calculation of the coefficient of variation of methylation for each tile in EPP and in TC populations revealed a mean CV of 9.15% for EPP and 4.38% for TC. The mean of differential methylation is -14.35% in EPP compared to TC (mean q-value of 9.975e-04), with a maximum of differential methylation of 91.95% (hypermethylated) and a minimum of -100.00% (hypomethylated) at the region level in EPP compared to TC. In a total of 42 024 differentially methylated tiles between the populations, 1 780 are significantly differentially methylated with the defined thresholds. This means that 4.236% of the tiles are significantly differentially methylated between EPP and TC populations on the reverse strand of DNA for the gonad tissue. The mean of hypermethylated DMR is 27.46% (q-value= 1.115e-03), and the mean of hypomethylated DMR is -21.60% (q-value= 9.771e-04) between the two populations, using the same threshold parameters.

3.4 | Gene-specific DNA methylation study by pyrosequencing

Four runs of pyrosequencing were performed in total targeting the sequences described in the **annexes 2 & 3**, each run testing for 24 samples. For the sequences DNMT3a_2 and MeCP2_2_2, only one replicate for each developmental stage pool was tested. Unfortunately, pyrosequencing of EPP population for MeCP2_2_2 didn't work (except for one replicate of the gastrula stage) as well as the unique OL replicate for TC population. This ultimately means that MeCP2_2_2 is represented by one replicate of the gastrula stage for EPP and TC, and three replicates for the 27th stage of TC. Additionally, only two replicates for the OL stage were kept for MeCP2_1. An example of a resulting pyrogram from a pyrosequencing run can be visualized in **annex 5**.

The global DNA methylation pattern in each sequence studied can firstly be observed in **figure 2**, which is regrouping the data of both EPP and TC populations. Notably, some methylation divergences can already be noticed within DNMT3a_3 and NIPBL sequences.

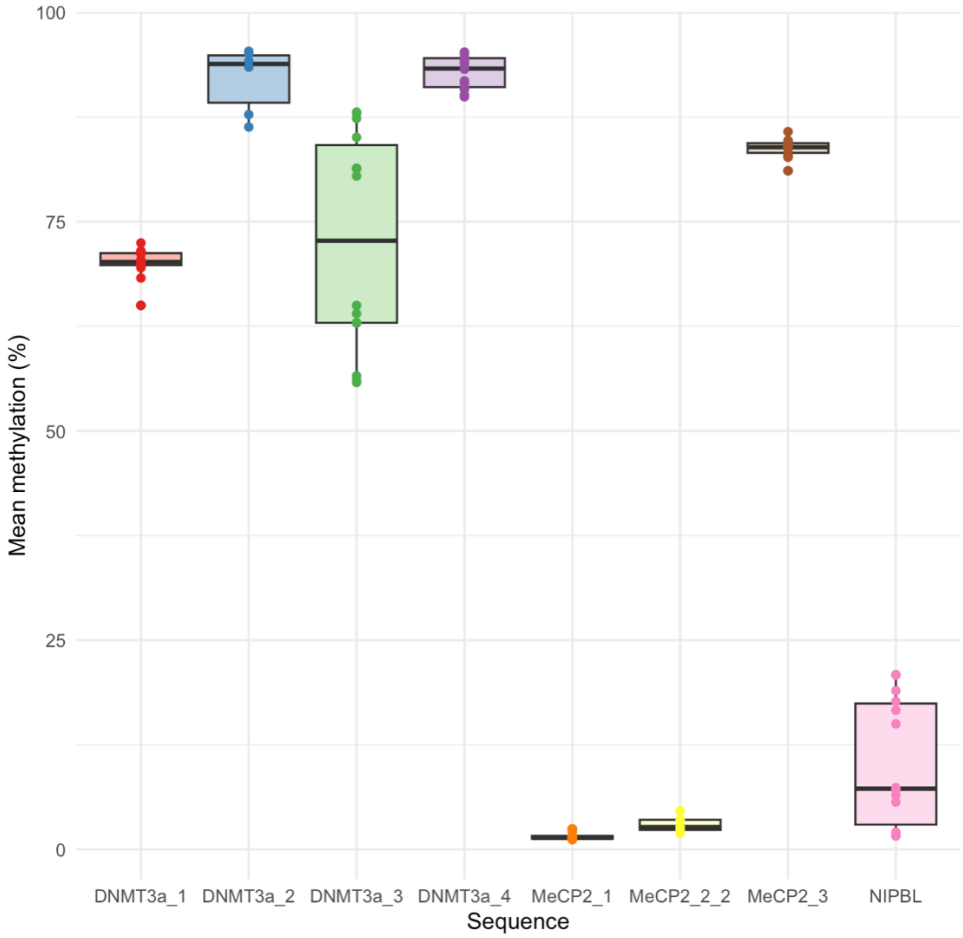

Figure 2: Boxplots demonstrating the mean methylation in percentage for each sequence of the genes studied, regrouping EPP and TC populations. Each sequence has been attributed a specific color. Each boxplot is represented by the replicates of a pool per developmental stage (3) and population (2). 1 gastrula pool= 20 eggs, 1 OL pool= 14 eggs, 1 27th pool= 7 eggs. Exception for the gastrula and OL stages of TC population: only 1 replicate (1 pool) of 15 eggs and 10 eggs respectively.

Each sequence was individually analyzed for its DNA methylation pattern in the diverse developmental stages for both populations. Following the above observations, DNMT3a_3 and NIPBL sequences were specifically scoped, and their methylation patterns are shown in **figure 3**. A demethylation is seen for DNMT3a_3, for both populations. NIPBL, on the other hand, demonstrates an increasing methylation throughout the advancement of the embryonic development of *K. marmoratus*, for both populations. These methylation percentages are well represented as all the replicates of a single developmental stage stick together.

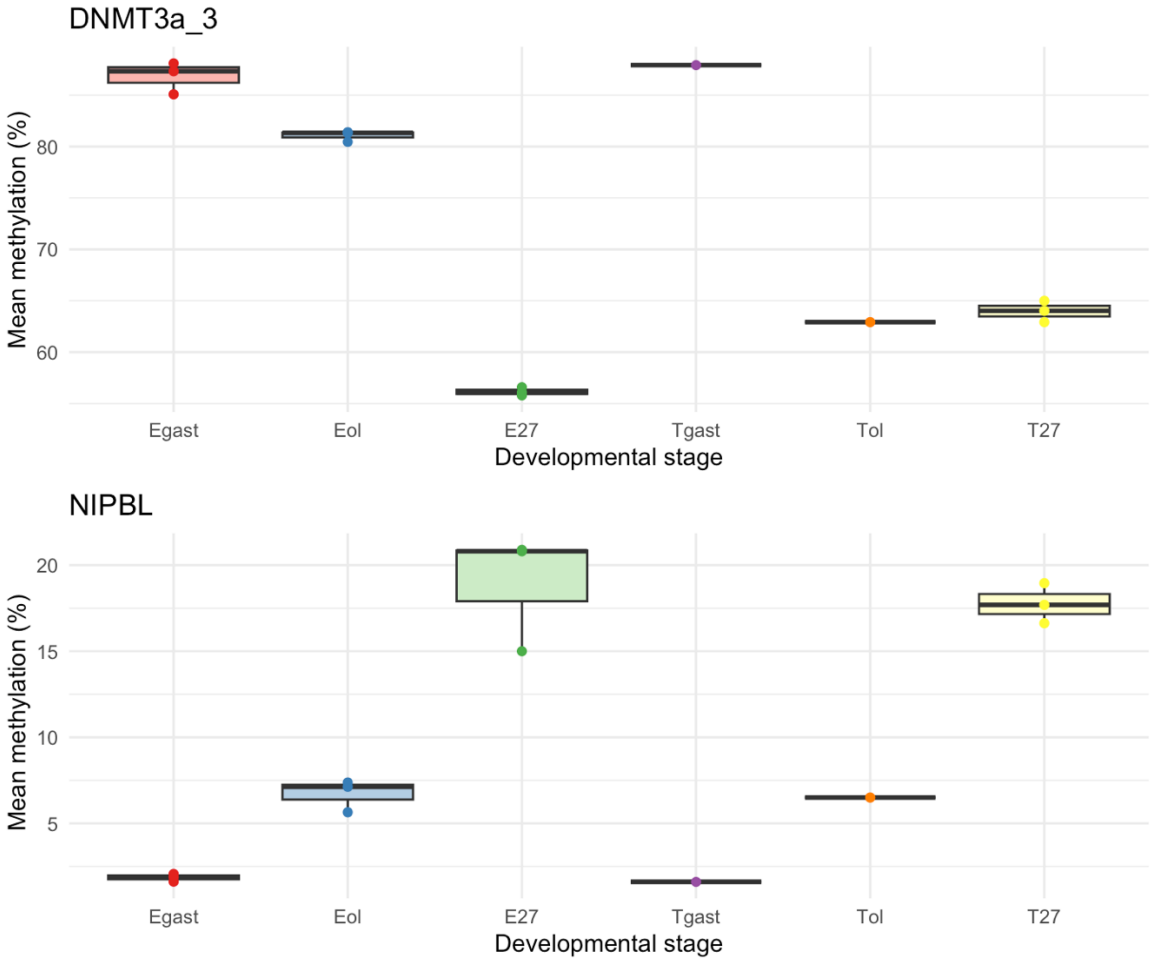

Figure 3: Boxplots showing the mean methylation in percentage specifically for DNMT3a_3 and NIPBL sequences in the diverse developmental stages, separating EPP (E) and TC (T) populations. Each developmental stage has been attributed a specific color. Gast= gastrula stage, ol= otic-lens formation, 27= 27th stage. Each boxplot is represented by the replicates of a pool per developmental stage (3). 1 gastrula pool= 20 eggs, 1 OL pool= 14 eggs, 1 27th pool= 7 eggs. Exception for the gastrula and OL stages of TC population: only 1 replicate (1 pool) of 15 eggs and 10 eggs respectively.

For the following figure **(Figure 4)**, the mean methylation of all the replicates of a developmental stage was calculated and used as data points for the representation of the methylation pattern throughout the chronology of the embryonic development of *K. marmoratus*. It is firstly observable that both populations tend to follow the same methylation pattern throughout the advancement of the embryonic development. Secondly, all sequences show relatively high methylation, except for MeCP2_1, MeCP2_2_2, and NIPBL which demonstrate much lower methylation following embryonic development. A slight demethylation throughout embryogenesis is observable for DNMT3a_2, and a more drastic demethylation is also remarkable for DNMT3a_3. Conversely, NIPBL demonstrates considerable increasing methylation following embryogenesis.

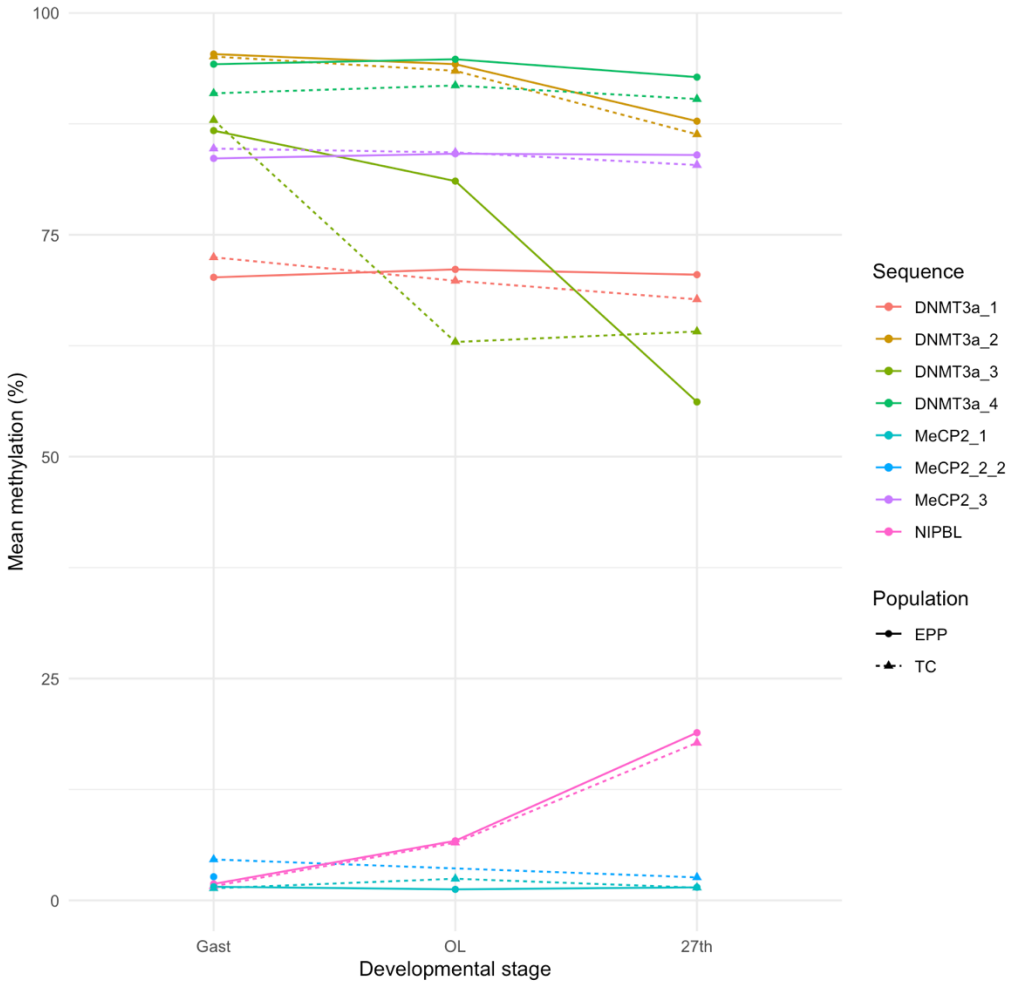

Figure 4: Representation of the mean methylation in percentage of each sequence for the three developmental stages following the chronology of development of *K. marmoratus*, separating EPP and TC populations. Each sequence has been attributed a specific color. Full lines with a round shape represent EPP population, whereas dashed lines with a triangular shape represent TC population. Gast= gastrula stage, OL= Otic-Lens formation, 27^{th}= 27^{th} stage. Standard deviations are expressly not shown to avoid overlapping between each data point, however their values are described in **annex 6**. Each data point represents the mean methylation of the replicates of a pool per developmental stage (3). 1 gastrula pool= 20 eggs, 1 OL pool= 14 eggs, 1 27^{th} pool= 7 eggs. Exception for the gastrula and OL stages of TC population: only 1 replicate (1 pool) of 15 eggs and 10 eggs respectively.

A more precise analysis was also realized on the CpG level. The methylation pattern of each CpG passing the manual interpretation of the pyrograms was examined for every sequence. Among these sequences, several CpGs were particularly retained for their remarkable methylation pattern, and a description of each one of them is available in **table 1**.

Sequence	Retained CpG	Remarkable pattern
DNMT3a_1	**CpG 3** Position 3: -2 677bp	Less methylation (around 46%) than the first two CpGs for this sequence (around 80%) for both populations
	CpG 4 Position 4: -2 633bp	Similar methylation for all stages of EPP and Tgast* (around 71%, already lower than the first two CpGs of this sequence), however lower methylation for Tol* and T27 (around 64%)
DNMT3a_2*	**CpG 1, 4, 5, 7** Position 1: +3 657bp Position 4: +3 666bp Position 5: +3 717bp Position 7: +3 776bp	Visible demethylation (around 98%) from the gastrula stage to the 27th stage (around 90%) for both populations
DNMT3a_3	**CpG 1, 2, 3, 4, 5, 6** Position 1: +7 499bp Position 2: +7 518bp Position 3: +7 529bp Position 4: +7 535bp Position 5: +7 551bp Position 6: +7 568bp	Visible demethylation (around 90%) from the gastrula stage to the 27th stage (60%) for both populations
DNMT3a_4	**CpG 1, 2, 3, 4, 7, 8** Position 1: +32 838bp Position 2: +32 852bp Position 3: +32 857bp Position 4: +32 867bp Position 7: +32 906bp Position 8: +32 928bp	Visible demethylation from the gastrula stage (98%) to the 27th stage (94%) for both populations
	CpG 9 Position 9: +32 934bp	CpG clearly defined by all the replicates (little variation for both populations) + Egast (86%) and Tgast* (64%) have distinct methylations
MeCP2_3	**CpG 2** Position 2: +4 568bp	100% methylation for every developmental stage of both populations
	CpG 6 Position 6: +4 619bp	Lower methylation (around 52%, compared to other CpGs of around 89% except for CpG 2) for all developmental stages of both populations
	CpG 8 Position 8: +4 631bp	Lower methylation (around 75%, compared to other CpGs of around 89% except for CpG 2) for all developmental stages of both populations
NIPBL	**CpG 1, 2, 3, 5, 6, 7, 11** Position 1: -358bp Position 2: -351bp Position 3: -344bp Position 5: -333bp Position 6: -329bp Position 7: -313bp Position 11: -291bp	Increasing methylation from around 3% (gast), passing by around 7% (OL) to around 20% (27th) in both populations
	CpG 4 Position 4: -337bp	Increasing methylation from around 3% (gast), passing by around 10% (OL) to around 33% (27th) in both populations
	CpG 8, 9, 10 Position 8: -306bp Position 9: -304bp Position 10: -298bp	Lower methylation for the gastrula stage (around 2%), OL (3.5%) and the 27th stage (around 8%) in both populations

Table 1: Individual CpGs for which a remarkable methylation variation was observed in the sequences studied. The position of each focused CpG is described based on the +1 transcription starting site of the gene, and the noticeable methylation pattern is detailed. *Only one replicate. bp= base-pair; E= EPP population, T= TC population; gast= gastrula stage, OL= Otic-Lens formation, 27^{th}= 27^{th} stage.

Concerning the statistical tests performed on each sequence individually, the mean methylation was tested as response variable and the developmental stage was defined as the explanatory variable. Because EPP was the only population where all the replicates (in number and in pyrosequencing quality validation, except for MeCP2_2_2) were encountered, the statistical tests were executed uniquely on this population. Significant results from the diverse tests were observed for DNMT3a_3, DNMT3a_4, and NIPBL, and are shown in **table 2**.

Sequence	Population	Test performed	Statistical result (in p-value)
DNMT3a_3	EPP	Kruskal-Wallis	p= 0.02732
		Dunn's post-hoc test	Egast-E27: p= 0.0109*
		GLM quasibinomial	Egast (Intercept): p= 1.85e-08 *** Eol: p= 0.000497 *** E27: p= 1.34e-07 ***
		ANOVA II (from above model)	p < 2.2e-16 ***
DNMT3a_4	EPP	ANOVA II	p= 0.04712 *
NIPBL	EPP	Bartlett's test	p= 0.01781
		One-way ANOVA	p= 0.00013 ***
		Tukey post-hoc test	Egast-E27: p-adj= 0.0001208 Eol-E27: p-adj= 0.0007870
		GLM quasibinomial	Egast (Intercept): p= 2.81e-06 *** Eol: p= 0.00247 ** E27: p= 5.56e-05 ***
		ANOVA II (from above model)	p < 2.2e-16 ***

Table 2: Significant statistical results performed on the sequences' dataframes. Each test type is described with its associated significant result. All tests were executed on EPP population. P-values have a significance threshold of 0.05 (except for Dunn's test where $p \leq 0.025$). The more asterisks are added to the p-value, the most significant is the result. For the GLM quasibinomial test, the mean ratio (proportion) of methylation of the gastrula stage was used for comparison (intercept) with other stages. Nothing significant was found for DNMT3a_4 GLM quasibinomial test. E= EPP; gast= gastrula stage, ol= otic-lens formation, 27= 27^{th} stage.

4 | Discussion

| Cytosine context distribution in EPP and TC populations on the reverse strand of DNA in the gonads

This work reports a predominant cytosine distribution in CHH context (53%), followed by CHG context (26%), CpG context (21%) and finally the unknown context (CN or CHN, 1%) in both populations. **Chapelle (2023)** studied the brains of two hermaphroditic Floridian (including EPP) and two hermaphroditic Belizean (including TC) populations of the mangrove rivulus and showed very close results (55% cytosines in CHH context, 24% in CHG context, and 21% in CpG context). The reverse strand of DNA in the gonads thus seems to have a similar distribution of cytosines to the brain tissue. When regrouping all populations studied, **Chapelle (2023)** also reported an average of 65.11% methylation for cytosines in CpG context, 1.4% methylation in CHH and 1.1% methylation in CHG contexts. **Madarasz (2023)** also studied the brain methylome of hermaphrodite EPP population and reported similar methylation percentages either in CpG, CHH, and CHG contexts. **Voisin *et al.* (2022)** performed RRBS analysis on the liver tissue of another hermaphroditic Floridian population, DC4 (Dove Creek). They demonstrated between 63.5% and 66.4% of CpG methylation and between 1.7% and 2.4% of non-CpG methylation (after treatment with 17-α-ethinylestradiol (EE2)). Therefore, the methylation pattern observable in non-CpG contexts seems analogous to diverse tissues of *K. marmoratus*, even though it remains slightly higher in the gonads. However, around 10% higher methylation in CpG context is reported in the gonads compared to the liver and brain tissues. Epigenetics, in this case DNA methylation, is known to be tissue-dependent **(Ohgane *et al.*, 2008)**. The tissue-specificity of DNA methylation is thus relatively outlined between the gonads, the brain and the liver, mainly within a CpG context. The methylation percentages in every context studied are homogeneous between EPP and TC populations, hence no methylation specificities can be underlined, at least for the reverse strand of DNA in the gonads. The reverse strand, also called the non-coding strand, is the template for transcription. As DNA methylation is commonly associated with gene expression repression, the relatively higher methylation pattern observed within the gonads would thus promote a greater transcriptional repression within this tissue. **Fellous *et al.* (2018)** significantly showed very low mRNA expression of *TET1/2/3* (Ten-Eleven Translocation) in the gonads of hermaphroditic rivulus from Dove Creek (Florida). This finding corresponds with the results presented here as TET enzymes (1, 2, and 3) oxidize 5mC to promote DNA demethylation and collaborate with chromatin modifiers to regulate gene expression **(Chrysanthou *et al.*, 2022)**.

| DMC analysis for EPP and TC populations on the reverse strand of DNA in the gonads

A much higher mean of the coefficient of variation within EPP (32.13%) compared to TC (5. 62%) is reported, thus EPP apparently has more total variability of methylation at a single CpG level in the gonads. This is particularly intriguing as these two populations exhibit a distinct genetic background, where EPP population is represented by consistent selfing whereas TC has higher outcrossing rates with males, therefore enhancing genetic diversity **(Tatarenkov *et al.*, 2015; Chapelle, 2023)**. This pattern raises relevant questioning towards phenotypic plasticity of EPP population. An interesting phenotypic trait observed by **Chapelle (2023)** was

that individuality (consistent among individual behavioral variation) appeared for EPP and another Floridian population, but not in the most genetically diverse population from Belize. Knowing that epigenetic mechanisms are directly affected by the environment **(Daxinger & Whitelaw, 2010; Chapelle & Silvestre, 2022)**, a higher variation of DNA methylation within EPP population in the tissue producing the gametes for subsequent generations would need serious further investigation. **Chapelle (2023)** reported a CV of 48.86% in EPP and of 60.26% in TC in the brain and described it as a synthetic view of epigenetic diversity in each population for a given tissue. There appears to be once again a divergence between the brain and the gonadal tissue, here concerning single-CpG coefficient of variation, as EPP and TC demonstrate a lower CV in the gonads than in the brain. A particularly drastic difference is observable for TC population. This is an interesting pattern, knowing that epigenetics is tissue-dependent **(Ohgane *et al.*, 2008)**. It is important to keep in mind that for techniques such as RRBS, where millions of CpG sites are studied, investigation of every single CpG as an independent unit of analysis can considerably increase the false discovery rate **(Chatterjee *et al.*, 2017)**. This is because variation at single sites is greater than the one of a contig of sites since the relatively lower coverage per site increases variation **(Ehrlich & Lacey, 2013)**. However, only 1.230% of the CpGs are significantly differentially methylated between EPP and TC populations, which is very low though. This means that CpG methylation variation is higher at an individual population level, especially concerning EPP, but significantly differentially methylated CpGs between the two populations remain apparently low.

| DMR analysis for EPP and TC populations on the reverse strand of DNA in the gonads

CV between the populations is more similar in the tile analysis, which is statistically more relevant, with 9.15% for EPP and 4.38% for TC. Knowing that there are presumably less tiles than CpGs in the portion of the genome analyzed after RRBS, it is interesting to mention that even though the total number of tiles selected as differentially methylated is inferior that the one of CpGs, the amount of significantly differentially methylated tiles is higher than the one of CpGs. Reported functionally relevant findings have been generally associated with genomic regions rather than single-CpGs, therefore research for association at the region level as opposed to the single-CpG level is recommended **(Jaffe *et al.*, 2012)**. EPP's CV remains a bit higher, however this analysis might highlight outliers that were encountered in single-CpG analysis. From a tile perspective, there would be a lot less methylation variation within EPP population. Only 4.236% of the tiles are found significantly differentially methylated between EPP and TC populations, which is quite low as well. DMR analysis thus demonstrates little methylation divergence in the gonads within and between populations of *K. marmoratus* having a different genetic profiling, particularly on the reverse strand of DNA, independently from the selfing rate. In the brain, **(Chapelle, 2023)** reported only 687 (1.18%) of the 300bp methylated regions (116 190 in total) as significantly differentially methylated for EPP against each of the three other populations (regrouping every comparison against EPP). Only 647 (1.12%) of the 300bp methylated regions were significantly differentially methylated for TC against each of the three other populations. The gonads thus seem to have a bit more significantly differentially methylated tiles between only two populations. Tissue-specificity of DNA methylation is once again highlighted here. It appears that

there isn't much differential methylation between mangrove rivulus populations, even with a different coverage per tile (10x for the brain and 3x here), at least for the brain and gonads, and even with a distinct genetic variability.

| Global methylation pattern from pyrosequencing sequences

First and foremost, it appears that DNMT3a_2 (1st intron of *DNMT3a*) and DNMT3a_4 (5th exon of this gene) are the most methylated sequences, whereas MeCP2_1 (promoter) and MeCP2_2_2 (1st intron) are the least methylated ones for all the sequences studied **(Figure 2)**. Nevertheless, the results of DNMT3a_2 should be interpreted cautiously as only one replicate for each developmental stage was encountered for analysis. It is known in vertebrates that gene bodies including introns and exons are often methylated, whereas CpGs in the gene promoter region are commonly poorly methylated **(Saxonov *et al.*, 2006; Suzuki & Bird, 2008; Hon *et al.*, 2013)**. The function of gene body methylation is still discussed, however it is proposed to suppress gene expression by promoting chromatin densification **(Deaton *et al.*, 2011)** and interacting with functional elements in transcribed regions, including enhancers, alternative promoters, TF binding sites, and repetitive elements **(Yang *et al.*, 2014)**. Gene body methylation appears to be closely related to cell development and differentiation and would play a key developmental regulatory role **(Wang *et al.*, 2022)**. Cytosine methylation for *K. marmoratus* follows the above patterns, as gene bodies (introns and exons) are typically methylated, whereas CpGs in the gene promoter region are lowly methylated without any significant differences between either populations having great genetic variability and clonal populations **(Chapelle, 2023)**. **Goujon (2019)** analyzed RRBS results on the same three developmental stages. He measured the proportion of the fragments being characterized as hypermethylated (methylation > 0.85) and hypomethylated (methylation < 0.15) for the developmental stages, given their genomic position. The majority of the hypermethylated fragments were located within the genes whereas hypomethylated fragments were found within promoter regions. Additionally, no significant difference for the fragments' distribution has been observed between the three stages for the hyper- or hypomethylated conditions **(Goujon, 2019)**. Hence, the methylation patterns of DNMT3a_2, DNMT3a_4, and MeCP2_1 seem to follow the known DNA methylation characteristics of introns, exons, and promoter regions for vertebrates. MeCP2_2_2 doesn't follow the awaited methylation pattern of introns, but nothing can really be deducted from this sequence due to a lack of replicates for the diverse developmental stages and for the populations. DNMT3a_1 represents the promoter of *DNMT3a*, which shows relatively high methylation, and is the lowest methylated sequence of *DNMT3a*. This pattern challenges the commonly accepted methylation state of promoters, arguing that the expression of this gene would be repressed since gene body methylation is positively correlated with transcriptional activity in most animal species **(De Mendoza *et al.*, 2020)** and DNA methylation of regulatory regions is typically associated with silencing **(Feng *et al.*, 2010; Spainhour *et al.*, 2019; Peixoto *et al.*, 2020; Rauluseviciute *et al.*, 2020)**. This can firstly be explained by the fact that promoter methylation is often highly dynamic during development **(Suzuki & Bird, 2008)**, and that *DNMT3a*'s primary action, in mammals, is methylating a set of genes at the late stages of embryonic development, especially after birth **(Smith & Meissner, 2013; Li &**

Zhang, 2014). Interestingly, a comparative mapping of *DNMT3a* related genes showed that this gene is in a region of conserved synteny between zebrafish and other fish species, and more globally other vertebrates **(Campos *et al.*, 2012)**. **Fellous *et al.* (2018)** demonstrated that the gastrula and OL stages didn't show *DNMT3a* mRNA expression, however a slight expression was measured for the 27th stage. This up-regulation of *DNMT3a* mRNA from OL until hatching is similar to other fish **(Fang *et al.*, 2013; Dasmahapatra & Khan, 2015; Firmino *et al.*, 2017)** where this gene is interestingly implicated in lens formation **(Seritrakul & Gross, 2014)** (thus representing the 19th stage of **Mourabit *et al.* (2011)** included in OL), in neurogenesis **(Firmino *et al.*, 2017)** (in relation with the 18th stage of **Mourabit *et al.* (2011)**, the otic vesicle formation, also included in OL), and organogenesis **(Takayama *et al.*, 2014)**. Based on these results (like zebrafish **(Campos *et al.*, 2012)**, **Fellous *et al.* (2018)** suggested that a certain level of erasure and repatterning of *de novo* CpG DNA methylation might be taking place later during the re-methylation phase (starting towards the 100% epiboly stage) with *DNMT3a*. These results seem to correlate with the methylation state of DNMT3a_1 found in this work. A slight divergence in the populations' methylations is also visible for the gastrula and the 27th stages of this gene. Interestingly, data points for DNMT3a_3 (the 2nd intron of *DNMT3a*) are dispersed through a range of methylation percentages, showing distinct methylation patterns following embryogenesis. This sequence indeed demonstrates a remarkable stage by stage demethylation while progressing through development **(Figure 4)**. Every statistical test performed on DNMT3a_3 for EPP population showed a significant result when testing the effect of the developmental stage on the mean methylation **(Table 1)**. A particularly meaningful result was observed when comparing the mean methylation of the gastrula stage with the 27th stage when performing a Dunn's pairwise comparison of means post-hoc test. In addition, the GLM quasibinomial also demonstrates significant results when comparing the gastrula stage (intercept) with the two other stages of development. The first two introns (DNMT3a_2 and DNMT3a_3) of *DNMT3a* thus exhibit progressive demethylation while advancing in embryogenesis, with DNMT3a_3 having already less methylation than the first intron, for all stages studied here. This seems to match again with the previous observations, as progressive demethylation towards the 27th stage would allow higher transcription rates of *DNMT3a*, gradually giving access of the transcriptional machinery to the sequence. Furthermore, two main divergences emerge in the methylation state between EPP and TC populations for DNMT3a_3 and DNMT3a_4 **(Figure 4)**. For the first sequence, EPP shows 18% more methylation than TC for the OL stage, and 8% less methylation than TC for the 27th stage, demonstrating an interesting distinct pattern between two genetically different populations of the mangrove rivulus. DNMT3a_4 shows no significant result when comparing the developmental stages' effect on the mean methylation in the GLM model. This is justified by a slight separation between two sets of data points representing both populations **(Figure 2)** where a 4% lower methylation is visible during all the development for TC **(Figure 4)**. Nevertheless, the developmental stages of EPP globally still have a significant effect on the mean methylation when performing an ANOVA II **(Table 2)**. Unfortunately, due to a lack of replicates for certain stages of TC, no population effect was tested on these sequences.

MeCP2 sequences demonstrate extremely low methylation, except for MeCP2_3, which is the 3rd exon of this gene, with a similar methylation display between the populations. This high methylation state of an exon follows the common methylation pattern of this genomic region. The promoter region (MeCP2_1) is the lowest methylated sequence studied in this work, showing that the promoter region is hypomethylated, following the familiar expected methylation state of promoters, and that the gene is very likely expressed throughout all the advancement of the embryonic development of *K. marmoratus*. MeCP2 has a methyl-DNA-binding domain, therefore it may influence chromatin compaction and thus the transcriptional activity of a genomic region, as DNA methylation is typically associated with transcriptional repression **(Lindeman *et al.*, 2010; Liang *et al.*, 2011; Song *et al.*, 2014)**. **Fellous *et al.* (2018)** demonstrated a dynamic expression pattern of *MeCP2* particularly in the late stages of development, specifically starting at the heartbeat stage (20th stage in **Mourabit *et al.* (2011)**, thus just after OL). They proposed the implication of this gene into neurogenesis, alike *Danio rerio*, where this protein regulates neural cell differentiation **(Gao *et al.*, 2015)**, and is needed for correct axonal elongation of motor neurons and synapse formation **(Nozawa *et al.*, 2017)**. In this study however, the data points in **figure 2** are sticking together for *MeCP2* sequences, showing little variation in the methylation state throughout the three embryonic stages. This aggregation matches the close mRNA expression of this gene for the three studied stages reported in **Fellous *et al.* (2018)**, however *MeCP2* expression was very low for these stages, contradicting the low methylation pattern observed in this work that would promote mRNA expression. Nevertheless, the 3rd exon of *MeCP2* (MeCP2_3) demonstrates high methylation, a state often expected for exons, and for all developmental stages. Altogether, a differential correlation between transcriptional repression by DNA methylation (studied in this work) and the actual gene expression pattern (reported by **Fellous *et al.* (2018)**) can eventually be proposed for *MeCP2*. Certain genes show no correlation between their methylation states and their expression profiles, *MeCP2* appears to be one of them. This opens hypotheses towards the possible requirement of other regulatory elements such as enhancers into *MeCP2* transcription, as they activate transcription of a gene to higher levels than it would be the case in their absence **(Pennacchio *et al.*, 2013)**. Enhancers function at distance by forming chromatin loops to bring the enhancer and target gene into proximity **(Krivega & Dean, 2012)**. Further investigation on other exons would be needed to come to a better idea of the effective transcription pattern of *MeCP2*.

Lastly, *NIPBL* also exhibits interesting results as data points, likewise DNMT3a_3, are displaying various methylation percentages related to the developmental stages studied **(Figure 2)**. This is explained by the increasing methylation status of this promoter sequence while progressing through embryogenesis for both populations **(Figures 3 & 4)**. Furthermore, even if the methylation state increases, the pattern remains relatively poorly methylated, guiding for an access of the transcriptional machinery towards reading this gene, specifically in the earliest stages here (gastrula and OL) as there is an increasing methylation towards the 27th stage. These results match with **Voisin *et al.* (2022)** who measured changes in DNA methylation following developmental exposure to EE2 (17-α-ethinylestradiol). They significantly showed that only *NIPBL* promoter region with low methylation of 19.6% in the control group remarkably increased its methylation state to 41.5%

after exposure to 4 ng/L of EE2 in the liver tissue. NIPBL is a cohesin-loading factor and has an important regulatory role in the maintenance of 3D genome organization and function by interacting with numerous factors (*e.g.*, cohesin complex component) **(Gao *et al.*, 2019)**. Cohesin folds the genome in chromatin loops, holding sister chromatids together **(Alonso-Gil & Losada, 2023)**. The molecular functions therefore proposed by **Voisin *et al.* (2022)** associated with *NIPBL* encompass cell morphology and nervous system development and functioning. This methylation increase on the promoter region towards the end of embryogenesis raises critical questions on why this chromosome organizer and gene expression regulator would become downregulated. The present observations argue for a lower gradual need of NIPBL protein throughout the embryonic formation and temporary gene expression in the early stages. Moreover, plausible histone lysine demethylases (Kdm) and methyltransferases (Kmt) were identified by **Fellous *et al.* (2019)** for the mangrove rivulus. They found that the expression pattern of *Kdm* and *Kmt* during embryonic development was peaking in the gastrula stage whereas a reduction was observed in later embryogenesis. This seems to correlate with *NIPBL*'s genome organization function, as this gene becomes more methylated towards the end of embryogenesis. Finally, all statistical tests performed for NIPBL sequence showed significant results. Specifically, the Tukey multiple comparisons of means post-hoc test demonstrated significant p-adjusted values when testing the gastrula stage with the 27th stage, and the OL with the 27th stage. The GLM model showed significant results when comparing the gastrula stage (intercept) with OL and with the 27th stage.

| Individual CpG analysis by pyrosequencing

A few single-CpG methylation variation have been observed in this work **(Table 1)**, notably lower methylation than other CpGs of the same sequence (*e.g.*, DNMT3a_1 CpG 3 and CpG 4, MeCP2_3 CpG 6 and CpG 8), increasing methylation throughout embryogenesis (NIPBL CpG 4), or the highest possible methylation status (100%, MeCP2_3 CpG 2). These punctual variations raise questions whereas they exert a particular role in the overall gene expression status, or if they are stochastic methylation patterns not having any specific impacts. However, it remains particularly tricky to infer whatsoever concerning single-CpG methylation role, as on the one hand reported functionally relevant findings have been generally associated with genomic regions rather than single-CpGs **(Jaffe *et al.*, 2012)**, but **Lim *et al.* (2018)** showed the suppression of interferon-mediated anti-HBV response by single-CpG methylation. **Nile *et al.* (2008)** also demonstrated that the methylation status of a single CpG site in the *IL6* promoter is related to *IL6* mRNA levels and rheumatoid arthritis. On the other hand, epigenetic elements are probabilistic, interactive regulatory factors **(Adrian-Kalchhauser *et al.*, 2020)**. Measuring mRNA expression of the targeted sequences here could inform on the output of single-CpG methylation variation, especially in the promoter region. Single-CpG methylation was used to calculate the mean methylation for each replicate, therefore it is logical to see the data shown in **figures 2, 3, & 4** matching with the overall methylation state of CpGs in a given sequence.

| Evolutionary potential of DNA methylation in the two populations of *K. marmoratus*

RRBS analysis demonstrates a similar methylation pattern between EPP and TC populations within CpG, CHG, CHH and an unknown context. This result matches with DMC and DMR analyses, as few significantly differentially methylated CpGs and regions (1.230% and 4.236%, respectively) were identified between these two populations. These populations having a distinct genetic background seemingly demonstrate very low divergence in their methylation patterns within their gonads, either at a single CpG level and when considering regions of 300bp. These analyses procure fascinating insights, but most certainly raise crucial questions on the ultimate role of DNA methylation, if there is any, towards facing distinct self-fertilization rates in these populations. It is however important to mention that this analysis was only conducted on the reverse strand of DNA.

For a given genotype, the epigenetic variation could be environmentally induced or occur randomly **(Angers *et al.*, 2020; Biwer *et al.*, 2020)**. Pyrosequencing analysis has revealed a few divergences in the methylation state between EPP and TC populations at specific developmental stages of *K. marmoratus* **(Figure 4)**. The most intriguing methylation variation remains within DNMT3a_3 sequence. **Figure 3** reveals that EPP and TC methylation variations do not appear to be random, as all replicates analyzed stick together in the boxplots. Importantly, the population effect couldn't be statistically tested, therefore the following assumptions can be proposed but they remain purely hypothetical. In numerous eukaryotes, encompassing mammals, yeast, plants, and insects, introns can enhance gene expression without functioning as a binding site for transcription factors, a phenomenon called "intron-mediated enhancement" **(Shaul, 2017)**. The visible differences in the methylation state of DNMT3a_3 in EPP and TC raise the question on how and why the second intron of *DNMT3a*, located similarly in the same gene for the two populations, could have a distinct impact on a population *DNMT3a* expression. Introns can indeed increase transcript levels by affecting the rate of transcription, transcript stability, and nuclear export **(Shaul, 2017)**. If this phenomenon is applicable for *DNMT3a*, highlighting the necessity for further studies on the subject, the distinct methylation of the second intron would potentially differentially affect *DNMT3a*'s expression and its further implications. The evolutionary significance of the reprogramming event is questionable, it is hypothesized as a possible critical window arbitrating phenotypic plasticity as well as evolutionary adaptation to remarkably variable environments **(Fellous *et al.*, 2018)**. It would be interesting to study the methylation state of the other developmental stages to have a more accurate idea of the demethylation pattern of this sequence in both populations. Enlarging the studies on sequences of key epigenetic actors will probably give more awareness on the characteristics of each population's reprogramming step and draw further speculations on their adaptation to their environment. Except for DNMT3a_1, DNMT3a_3, and DNMT3a_4, all other sequences didn't demonstrate any variation between populations, alike **Chapelle (2023)** who didn't show any significant differences in the distribution of cytosine methylation (gene bodies and promoter) between populations having distinct genetic backgrounds in rivulus' brains.

Chapelle (2023), who designed the primers used in this work, did not show a significant effect of methylmercury (MeHg) on DNA methylation of targeted CpGs within the same sequences of interest, in 7 days post-hatching (dph) whole larvae and 90 dph adult brains. *DNMT3a*, *MeCP2* (except MeCP2_3), and *NIPBL* (particularly at the 27th stage) showed similar methylation states to the ones reported in this work (71.08 ± 2.58%, 2.21 ± 0.82%, and 23.65% ± 2.25%, respectively). The present study focuses on embryonic stages, therefore the similar methylation patterns observed in 7 dph larvae and 90 dph brains for the same analyzed sequences promote the stability of these epigenetic marks from the gastrula stage to the larva stage of *K. marmoratus*, even with a severe perturbator such as MeHg. Both research are complementary as the methylation pattern of the same sequences in larvae gives further ideas of the continuation of **figures 3 & 4**. The robustness of the methylation marks on those particular sequences might comfort the essentialness of these epigenetic actors towards the development of this fish, giving decisive understanding of the conserved methylation patterns that might be observed in nature. This is further supported by the identical methylation profiles seen in **figure 4** of most of the studied sequences for these genes, independently from the genetic differential background of a population. **Fellous *et al.* (2018)** indeed reported that the conserved domains and expression profiles of DNMT and MeCP2 proteins suggest that they play important roles during reproduction, gametogenesis and development. It is however once again highlighted that no population effect was tested in this work, such an analysis would be essential to stipulate further assumptions.

Single-CpG analysis has revealed several punctual DNA methylation variations in the studied sequences at specific developmental time points. It remains nonetheless particularly arduous to infer an evolutionary role from these variations. It is however interesting to highlight that stochastic epigenetic variations affect development and thus phenotype, therefore they may provide additional phenotypic diversity that could help natural populations facing a fluctuating environment **(Biwer *et al.*, 2020)**. Epigenetic variation is more prompt to have higher spontaneous rates of mutation than genetic variation, and has enhanced sensitivity reaction to environmental stimuli, possibly providing the raw material for phenotypic selection when genetic variation is scarce **(Drake *et al.*, 1998; Ossowski *et al.*, 2010; Becker *et al.*, 2011; Schmitz *et al.*, 2011; Zhang *et al.*, 2013)**.

Lastly, RRBS and pyrosequencing studies which focus on a very distinct genomic scale, seem to correspond on the methylation patterns between EPP and TC populations. These analyses indeed demonstrate very little variation in methylation between these two populations (except for DNMT3a_3), either during embryogenesis and at an adult, sexually mature state. Such dual approach seems to be of great complementation and would definitely be recommended for further research on any area studying epigenetics.

| Enhancement of the study and perspectives

First and foremost, it is most important to mention that RRBS study was only performed on the reverse (template) strand of DNA in the gonad tissue, this is due to a restricted time for analysis of the sequencing data. Therefore, the methylation pattern on the coding strand isn't known yet. Acquiring the methylation state

on the coding strand will allow to conduct a complete methylation analysis in the gonads. It will also permit, based on significantly identified DMRs, a visualization and annotation with the nearest genomic feature, and a functional enrichment on DMRs falling within gene bodies against the Gene Ontology database. Furthermore, a cluster analysis and a Principal Component Analysis (PCA) couldn't be realized in this work, as both analyses are only applicable on a matrix with no NA (Not Available). There were apparently NAs and NaNs (Not a Number) in the unite object used for such analyses. Clustering and PCA analyses would give visual ideas of the relationship between the methylation states of the samples and the populations. This would procure an ideal support for the justification or not of the similar methylation patterns observed between EPP and TC populations.

Pyrosequencing statistical results are only relevant for EPP population, however given the overall similar methylation pattern of both populations seen in **figure 4** (except for DNMT3a_1, DNMT3a_3, and DNMT3a_4), close results might be awaited for TC population. Enhancements preconized for this study include an increased number of replicates of each developmental stage, making the results presented here more accurate, but it demands more egg collection time. This could help elucidate the population divergences seen in DNMT3a_1, DNMT3a_3, and DNMT3a_4, and allow for the test of population effect on the mean methylation of the sequences. Moreover, even though **Chapelle (2023)** has provided the methylation states of *DNMT3a* and *NIPBL* in larvae and adult brains, this output was obtained after MeHg treatment. It would be interesting to see until when (through the timeline of embryonic development) the demethylation of DNMT3a_3 would go, alike the increasing methylation of NIPBL, to give accurate ideas of the ultimate expression profiles of these genes. Related work targeting more developmental stages and more sequences of key epigenetic actors would become handy for understanding their roles and functions, especially in a unique vertebrate model like the mangrove rivulus which brings the exceptional opportunity to scope epigenetic mechanisms. This study reveals interesting methylation status changes, in a timescale of hours post-fecundation. It therefore shows the dynamism of DNA methylation in a real-time perspective. Realizing a similar study with eggs collected from the field for all populations would give more realistic ideas on the patterns and evolutionary potentials of the methylation state of the targeted genes. The test for the population effect on the methylation status of the studied genes would therefore also bring more concrete assessments on a possible evolutionary role of DNA methylation on fundamental epigenetic actors.

Even though DMC analysis focuses on a restricted portion of the genome, its scoping scale is still a lot larger than individual CpG analysis from pyrosequencing. Therefore, searching for the methylation state of specific CpGs in sequences of major epigenetic contributors can give a sharper and additional view of the methylation configuration of a given tissue.

5 | Conclusion

This work procures interesting methylation patterns both in a restricted portion of the genome in the gonad tissue and at a gene-specific level of major epigenetic actors. Using the mangrove rivulus as model species has allowed to specifically focus on DNA methylation, thus this work joins previous research on promoting this fish as model species in various research areas, including omics, to study phenotypic plasticity. RRBS study suggests few significantly differentially methylated CpGs and regions between two populations of *K. marmoratus* having distinct genetic profiles, only on the reverse strand of DNA in the gonad tissue. Pyrosequencing study reveals intriguing methylation states on key epigenetic actors themselves, specifically on the intron level of *DNMT3a* and on the promoter region of *NIPBL*, proposing further research on the role of intron methylation towards gene expression and the contribution of *NIPBL* in the overall chromatin structure, as this sequence shows similar results to anterior research in the laboratory. Together, these analyses promote investigation of gonadal tissue on the one hand, as it is a particularly interesting tissue to tackle for studying phenotypic plasticity in populations of *K. marmoratus* with different genetic diversities. On the other hand, this work invites for more research on the regulation of major epigenetic contributors, specifically in this fish, as it can certainly give crucial insights of their roles and expressions in vertebrates. Combining techniques scoping distinct genomic scales can certainly further clarify evolutionary potentials in this fish.

References

Adrian-Kalchhauser, I., Sultan, S.E., Shama, L.N.S., Spence-Jones, H., Tiso, S., Keller Valsecchi, C.I., & Weissing, F.J. (2020). Understanding "Non-genetic" Inheritance: Insights from Molecular-Evolutionary Crosstalk. *Trends in Ecology & Evolution*, 35 (12), 1078-1089.

Akalin, A., Kormaksson, M., Li, S., Garrett-Bakelman, F.E., Figueroa, M.E., Melnick, A., & Mason, C.E. (2012). methylKit: a comprehensive R package for the analysis of genome-wide DNA methylation profiles. *Genome Biology*, 13 (10), R87.

Alonso-Gil, D., & Losada, A. (2023). NIPBL and cohesin: new take on a classic tale. *Trends in Cell Biology*, 33 (10), 860-871.

Ambrosi, C., Manzo, M., & Baubec, T. (2017). Dynamics and Context-Dependent Roles of DNA Methylation. *Journal of Molecular Biology*, 429 (10), 1459-1475.

Andrews, S. (2010). FastQC: A quality control tool for high throughput sequence data. Consulted on the 1st of January, 2024, on Babraham Bioinformatics: https://www.bioinformatics.babraham.ac.uk/projects/fastqc/.

Angers, B., Castonguay, E., & Massicotte, R. (2010). Environmentally induced phenotypes and DNA methylation: how to deal with unpredictable conditions until the next generation and after. *Molecular Ecology*, 19 (7), 1283-1295.

Angers, B., Perez, M., Menicucci, T., & Leung, C. (2020). Sources of epigenetic variation and their applications in natural populations. *Evolutionary Applications*, 13 (6), 1262-1278.

Becker, C., Hagmann, J., Müller, J., Koenig, D., Stegle, O., Borgwardt, K., & Weigel, D. (2011). Spontaneous epigenetic variation in the *Arabidopsis thaliana* methylome. *Nature*, 480 (7376), 245-249.

Biwer, C., Kawam, B., Chapelle, V., & Silvestre, F. (2020). The Role of Stochasticity in the Origin of Epigenetic Variation in Animal Populations. *Integrative and Comparative Biology*, 60 (6), 1544-1557.

Campos, C., Valente, L.M.P., & Fernandes, J.M.O. (2012). Molecular evolution of zebrafish *dnmt3* genes and thermal plasticity of their expression during embryonic development. *Gene*, 500 (1), 93-100.

Chapelle, V. (2023). Adaptation and evolution with low genetic diversity: a combined field and laboratory study on DNA methylation variation in the mangrove rivulus *Kryptolebias marmoratus* [Doctoral dissertation, University of Namur]. University of Namur Institutional Repository. https://pure.unamur.be/ws/portalfiles/portal/76232970/2023_ChapelleV_these_OA.pdf.

Chapelle, V., & Silvestre, F. (2022). Population Epigenetics: The Extent of DNA Methylation Variation in Wild Animal Populations. *Epigenomes*, 6 (4), 31.

Chatterjee, A., Rodger, E.J., Morison, I.M., Eccles, M.R., & Stockwell, P.A. (2017). Tools and Strategies for Analysis of Genome-Wide and Gene-Specific DNA Methylation Patterns. In: *Oral Biology: Molecular Techniques and Applications, Methods in Molecular Biology*, edited by Seymour, G.J., Cullinan, M.P., & Heng, N.C.K., 1537, pp 249-277, New York, NY, Springer New York.

Chrysanthou, S., Tang, Q., Lee, J., Taylor, S.J., Zhao, Y., Steidl, U., Zheng, D., & Dawlaty, M.M. (2022). The DNA dioxygenase Tet1 regulates H3K27 modification and embryonic stem cell biology independent of its catalytic activity. *Nucleic Acids Research*, 50 (6), 3169-3189.

Costa, W.J.E.M. (2011). Identity of Rivulus ocellatus and a new name for a hermaphroditic species of Kryptolebias from south-eastern Brazil (Cyprinodontiformes: Rivulidae). *Ichthyological Exploration of Freshwaters*, 22 (2), 185-192.

Dasmahapatra, A.K., & Khan, I.A. (2015). DNA methyltransferase expressions in Japanese rice fish (*Oryzias latipes*) embryogenesis is developmentally regulated and modulated by ethanol and 5-azacytidine. *Comparative Biochemistry and Physiology Part C: Toxicology & Pharmacology*, 176-177, 1-9.

Daxinger, L., & Whitelaw, E. (2010). Transgenerational epigenetic inheritance: More questions than answers. *Genome Research*, 20 (12), 1623-1628.

Deaton, A.M., Webb, S., Kerr, A.R.W., Illingworth, R.S., Guy, J., Andrews, R., & Bird, A. (2011). Cell type–specific DNA methylation at intragenic CpG islands in the immune system. *Genome Research*, 21 (7), 1074-1086.

De Mendoza, A., Lister, R., & Bogdanovic, O. (2020). Evolution of DNA Methylome Diversity in Eukaryotes. *Journal of Molecular Biology*, *Reading DNA Modifications*, 432 (6), 1687-1705.

Drake, J.W., Charlesworth, B., Charlesworth, D., & Crow, J.F. (1998). Rates of Spontaneous Mutation. *Genetics*, 148 (4), 1667-1686.

Earley, R.L., Hanninen, A.F., Fuller, A., Garcia, M.J., & Lee, E.A. (2012). Phenotypic Plasticity and Integration in the Mangrove Rivulus (*Kryptolebias marmoratus*): A Prospectus. *Integrative and Comparative Biology*, 52 (6), 814-827.

Ehrlich, M., & Lacey, M. (2013). DNA methylation and differentiation: silencing, upregulation and modulation of gene expression. *Epigenomics*, 5 (5), 553-568.

Ellison, A., Rodríguez López, C.M., Moran, P., Breen, J., Swain, M., Megias, M., Hegarty, M., Wilkinson, M., Pawluk, R., & Consuegra. S. (2015). Epigenetic regulation of sex ratios may explain natural variation in self-fertilization rates. *Proceedings of the Royal Society B: Biological* Sciences, 282 (1819), 20151900.

Fang, X., Thornton, C., Scheffler, B.E., & Willett, K.L. (2013). Benzo[a]pyrene decreases global and gene specific DNA methylation during zebrafish development. *Environmental Toxicology and Pharmacology*, 36 (1), 40-50.

Fellous, A., Earley, R.L., & Silvestre, F. (2019). The *Kdm/Kmt* gene families in the self-fertilizing mangrove rivulus fish, *Kryptolebias marmoratus*, suggest involvement of histone methylation machinery in development and reproduction. *Gene*, 687, 173-187.

Fellous, A., Labed-Veydert, T., Locrel, M., Voisin, A.S., Earley, R.L., & Silvestre, F. (2018). DNA methylation in adults and during development of the self-fertilizing mangrove rivulus, *Kryptolebias marmoratus*. *Ecology and Evolution*, 8 (12), 6016-6033.

Feng, S., Cokus, S.J., Zhang, X., Chen, P.Y., Bostick, M., Goll, M.G., Hetzel, J., Jain, J., Strauss, S.H., Halpern, M.E., Ukomadu, C., Sadler, K.C., Pradhan, S., Pellegrini, M., & Jacobsen, S.E. (2010). Conservation and divergence of methylation patterning in plants and animals. *Proceedings of the National Academy of Sciences*, 107 (19), 8689-8694.

Firmino, J., Carballo, C., Armesto, P., Campinho, M.A., Power, D.M., & Manchado, M. (2017). Phylogeny, expression patterns and regulation of DNA Methyltransferases in early development of the flatfish, *Solea senegalensis*. *BMC Developmental Biology*, 17 (1), 11.

Gao, H., Bu, Y., Wu, Q., Wang, X., Chang, N., Lei, L., Chen, S., Liu, D., Zhu, X., Hu, K., & Xiong, J.W. (2015). Mecp2 regulates neural cell differentiation by suppressing the Id1 to Her2 axis in zebrafish. *Journal of Cell Science*, 128 (12), 2340-2350.

Gao, D., Zhu, B., Cao, X., Zhang, M., & Wang, X. (2019). Roles of NIPBL in maintenance of genome stability. *Seminars in Cell & Developmental Biology*, *3D Genome and Diseases*, 90, 181-186.

Goll, M.G., & Bestor, T.H. (2005). Eukaryotic cytosine methyltransferases. *Annual Review of Biochemistry*, 74 (1), 481-514.

Goujon, V. (2019). Variabilité épigénétique durant le reprogramming chez le vertébré à autoféconda tion, *Kryptolebias marmoratus*. [Master's thesis, University of Namur]. University of Namur Institutional Repository.

https://pure.unamur.be/ws/portalfiles/portal/62847058/2019_VirgilioG_memoire.pdf.

Grossniklaus, U., Kelly, W.G., Ferguson-Smith, A.C., Pembrey, M., & Lindquist, S. (2013). Transgenerational epigenetic inheritance: how important is it? *Nature Reviews Genetics*, 14 (3), 228-235.

Harrington, R.W. (1961). Oviparous Hermaphroditic Fish with Internal Self-Fertilization. *Science*, 134 (3492), 1749-1750.

Heard, E., & Martienssen, R.A. (2014). Transgenerational Epigenetic Inheritance: Myths and Mechanisms. *Cell*, 157 (1), 95-109.

Herrel, A., Joly, D., & Danchin, E. (2020). Epigenetics in ecology and evolution. *Functional Ecology*, 34 (2), 381-384.

Hon, G.C., Rajagopal, N., Shen, Y., McCleary, D.F., Yue, F., Dang, M.D., & Ren, B. (2013). Epigenetic memory at embryonic enhancers identified in DNA methylation maps from adult mouse tissues. *Nature Genetics*, 45 (10), 1198-1206.

Hu, J., & Barrett, R.D.H. (2017). Epigenetics in natural animal populations. *Journal of Evolutionary Biology*, 30 (9), 1612-1632.

Jablonka, E., & Lamb, M.J. (1989). The inheritance of acquired epigenetic variations. *Journal of Theoretical Biology*, 139 (1), 69-83.

Jaffe, A.E., Murakami, P., Lee, H., Leek, J.T., Fallin, M.D., Feinberg, A.P., & Irizarry, R.A. (2012). Bump hunting to identify differentially methylated regions in epigenetic epidemiology studies. *International Journal of Epidemiology*, 41 (1), 200-209.

Kel, A.E., Gößling, E., Reuter, I., Cheremushkin, E., Kel-Margoulis, O.V., & Wingender, E. (2003). MATCH^{TM}: a tool for searching transcription factor binding sites in DNA sequences. *Nucleic Acids Research*, 31 (13), 3576-3579.

Kilvitis, H.J., Alvarez, M., Foust, C.M., Schrey, A.W., Robertson, M., & Richards, C.L. (2014). Ecological Epigenetics. In: *Ecological Genomics: Ecology and the Evolution of Genes and Genomes, Advances in Experimental Medecine and Biology*, edited by Landry, C.R., & Aubin-Horth, N., 781, pp 191-210, Dordrecht, Springer Netherlands.

Krivega, I., & Dean, A. (2012). Enhancer and promoter interactions-long distance calls. *Current Opinion in Genetics & Development*, 22 (2), 79-85.

Krueger, F. (2012). Trim Galore: A wrapper tool around Cutadapt and FastQC to consistently apply quality and adapter trimming to FastQ files, with some extra functionality for MspI-digested RRBS-type (Reduced Representation Bisulfite-Seq) libraries. Consulted on the 1st of January, 2024, on Babraham Bioinformatics: https://www.bioinformatics.babraham.ac.uk/projects/trim_galore/.

Krueger, F., & Andrews, S.R. (2011). Bismark: a flexible aligner and methylation caller for Bisulfite-Seq applications. *Bioinformatics*, 27 (11), 1571-1572.

Laland, K.N., Uller, T., Feldman, M.W., Sterelny, K., Müller, G.B., Moczek, A., Jablonka, E., & Odling-Smee, J. (2015). The extended evolutionary synthesis: its structure, assumptions and predictions. *Proceedings of the Royal Society B: Biological Sciences*, 282 (1813), 20151019.

Lamka, G.F., Harder, A.M., Sundaram, M., Schwartz, T.S., Christie, M.R., DeWoody, J.A., & Willoughby, J.R. (2022). Epigenetics in Ecology, Evolution, and Conservation. *Frontiers in Ecology and Evolution*, 10, 871791.

Li, L.C., & Dahiya, R. (2002). MethPrimer: designing primers for methylation PCRs. *Bioinformatics (Oxford, England)*, 18 (11), 1427-1431.

Li, H., Handsaker, B., Wysoker, A., Fennell, T., Ruan, J., Homer, N., Marth, G., Abecasis, G., & Durbin, R. (2009). The Sequence Alignment/Map format and SAMtools. *Bioinformatics*, 25 (16), 2078-2079.

Li, E., & Zhang, Y. (2014). DNA Methylation in Mammals. *Cold Spring Harbor Perspectives in Biology*, 6 (5), a019133.

Liang, P., Song, F., Ghosh, S., Morien, E., Qin, M., Mahmood, S., Fujiwara, K., Igarashi, J., Nagase, H., & Held, W.A. (2011). Genome-wide survey reveals dynamic widespread tissue-specific changes in DNA methylation during development. *BMC Genomics*, 12 (1), 231.

Lim, K.H., Park, E.S., Kim, D.H., Cho, K.C., Kim, K.P., Park, Y.K., Ahn, S.H., Park, S.H., Kim, K.H., Kim, C.W., Kang, H.S., Lee, A.R., Park, S., Sim, H., Won, J., Seok, K., You, J.S., Lee, J.H., Yi, N.J., Lee, K.W., Suh, K.S., Seong, B.L., & Kim, K.H. (2018). Suppression of interferon-mediated anti-HBV response by single CpG methylation in the 5′-UTR of *TRIM22*. *Gut*, 67 (1), 166-178.

Lindeman, L.C., Winata, C.L., Aanes, H., Mathavan, S., Alestrom, P., & Collas, P. (2010). Chromatin states of developmentally-regulated genes revealed by DNA and histone methylation patterns in zebrafish embryos. *The International Journal of Developmental Biology*, 54 (5), 803-813.

Madarasz, N. (2023). Epigenetic and behavioural variability in an isogenic lineage of *Kryptolebias marmoratus* during domestication under stable laboratory condition. [Master's thesis, Catholic University of Louvain-la-Neuve]. Dial.mem UCLouvain. https://dial.uclouvain.be/memoire/ucl/en/object/thesis%3A38789.

Martin, M. (2011). Cutadapt removes adapter sequences from high-throughput sequencing reads. *EMBnet. journal*, 17(1), 10-12.

Monk, M., Boubelik, M., & Lehnert, S. (1987). Temporal and regional changes in DNA methylation in the embryonic, extraembryonic and germ cell lineages during mouse embryo development. *Development*, 99 (3), 371-382.

Mourabit, S., Edenbrow, M., Croft, D.P., & Kudoh, T. (2011). Embryonic development of the self-fertilizing mangrove killifish *Kryptolebias marmoratus*. *Developmental Dynamics*, 240 (7), 1694-1704.

Nicoglou, A., & Merlin, F. (2017). Epigenetics: A way to bridge the gap between biological fields. *Studies in History and Philosophy of Science Part C: Studies in History and Philosophy of Biological and Biomedical Sciences*, 66, 73-82.

Nile, C.J., Read, R.C., Akil, M., Duff, G.W., & Wilson, A.G. (2008). Methylation status of a single CpG site in the *IL6* promoter is related to *IL6* messenger RNA levels and rheumatoid arthritis. *Arthritis & Rheumatology*, 58 (9), 2686-2693.

Nozawa, K., Lin, Y., Kubodera, R., Shimizu, Y., Tanaka, H., & Ohshima, T. (2017). Zebrafish Mecp2 is required for proper axonal elongation of motor neurons and synapse formation. *Developmental Neurobiology*, 77 (9), 1101-1113.

Ohgane, J., Yagi, S., & Shiota, K. (2008). Epigenetics: the DNA methylation profile of tissue-dependent and differentially methylated regions in cells. *Placenta*, 29, 29-35.

Okano, M., Bell, D.W., Haber, D.A., & Li, E. (1999). DNA Methyltransferases Dnmt3a and Dnmt3b Are Essential for De Novo Methylation and Mammalian Development. *Cell*, 99 (3), 247-257.

Ortega-Recalde, O., & Hore, T.A. (2019). DNA methylation in the vertebrate germline: balancing memory and erasure. Edited by Blewitt, M. *Essays in Biochemistry*, 63 (6), 649-661.

Ossowski, S., Schneeberger, K., Lucas-Lledó, J.I., Warthmann, N., Clark, R.M., Shaw, R.G., Weigel, D., & Lynch, M. (2010). The Rate and Molecular Spectrum of Spontaneous Mutations in *Arabidopsis thaliana*. *Science*, 327 (5961), 92-94.

Peixoto, P., Cartron, P.F., Serandour, A.A., & Hervouet, E. (2020). From 1957 to Nowadays: A Brief History of Epigenetics. *International Journal of Molecular Sciences*, 21 (20), 7571.

Pennacchio, L.A., Bickmore, W., Dean, A., Nobrega, M.A., & Bejerano, G. (2013). Enhancers: five essential questions. *Nature reviews. Genetics*, 14 (4), 288-295.

Perez, M.F., & Lehner, B. (2019). Intergenerational and transgenerational epigenetic inheritance in animals. *Nature Cell Biology*, 21 (2), 143-151.

Rauluseviciute, I., Drabløs, F., & Rye, M.B. (2020). DNA hypermethylation associated with upregulated gene expression in prostate cancer demonstrates the diversity of epigenetic regulation. *BMC Medical Genomics*, 13 (1), 6.

Russo, V.E., Martienssen, R.A., & Riggs, A.D. (1996). Epigenetic mechanisms of gene regulation. Cold Spring Harbor Laboratory Press.

Sadler, K.C. (2023). Epigenetics across the evolutionary tree: New paradigms from non-model animals. *BioEssays*, 45, e2200036.

Saxonov, S., Berg, P., & Brutlag, D.L. (2006). A genome-wide analysis of CpG dinucleotides in the human genome distinguishes two distinct classes of promoters. *Proceedings of the National Academy of Sciences*, 103 (5), 1412-1417.

Schmitz, R.J., Schultz, M.D., Lewsey, M.G., O'Malley, R.C., Urich, M.A., Libiger, O., Schork, N.J., & Ecker, J.R. (2011). Transgenerational Epigenetic Instability Is a Source of Novel Methylation Variants. *Science*, 334 (6054), 369-373.

Schrey, A.W., Richards, C.L., Meller, V., Sollars, V., & Ruden, D.M. (2012). The Role of Epigenetics in Evolution: The Extended Synthesis. *Genetics Research International*, 2012 (286164), 1-3.

Scott Taylor, D. (2012). Twenty-Four Years in the Mud: What Have We Learned About the Natural History and Ecology of the Mangrove Rivulus, *Kryptolebias marmoratus*? *Integrative and Comparative Biology*, 52 (6), 724-736.

Seritrakul, P., & Gross, J.M. (2014). Expression of the De Novo DNA Methyltransferases (*dnmt3* - *dnmt8*) During Zebrafish Lens Development. *Developmental Dynamics*, 243 (2), 350-356.

Shaul, O. (2017). How introns enhance gene expression. *The International Journal of Biochemistry & Cell Biology*, 91 (Pt B), 145-155.

Smith, Z.D., & Meissner, A. (2013). DNA methylation: roles in mammalian Development. *Nature Reviews Genetics*, 14 (3), 204-220.

Song, C., Feodorova, Y., Guy, J., Peichl, L., Jost, K.L., Kimura, H., Cardoso, M.C., Bird, A., Leonhardt, H., Joffe, B., & Solovei, I. (2014). DNA methylation reader MECP2: cell type- and differentiation stage-specific protein distribution. *Epigenetics & Chromatin*, 7 (1), 17.

Spainhour, J.C.G., Lim, H.S., Yi, S.V., & Qiu, P. (2019). Correlation Patterns Between DNA Methylation and Gene Expression in The Cancer Genome Atlas. *Cancer Informatics*, 18, 1-11.

Suzuki, M.M., & Bird, A. (2008). DNA methylation landscapes: provocative insights from epigenomics. *Nature Reviews Genetics*, 9 (6), 465-476.

Takayama, K., Shimoda, N., Takanaga, S., Hozumi, S., & Kikuchi, Y. (2014). Expression patterns of *dnmt3aa*, *dnmt3ab*, and *dnmt4* during development and fin regeneration in zebrafish. *Gene Expression Patterns*, 14 (2), 105-110.

Tatarenkov, A., Earley, R.L., Perlman, B.M., Scott Taylor, D., Turner, B.J., & Avise, J.C. (2015). Genetic Subdivision and Variation in Selfing Rates Among Central American Populations of the Mangrove Rivulus, *Kryptolebias marmoratus*. *Journal of Heredity*, 106 (3), 276-284.

Tatarenkov, A., Earley, R.L., Scott Taylor, D., & Avise, J.C. (2012). Microevolutionary Distribution of Isogenicity in a Self-fertilizing Fish (*Kryptolebias marmoratus*) in the Florida Keys. *Integrative and Comparative Biology*, 52 (6), 743-752.

Tatarenkov, A., Lima, S.M.Q., Scott Taylor, D., & Avise, J.C. (2009). Long-term retention of self-fertilization in a fish clade. *Proceedings of the National Academy of Sciences*, 106 (34), 14456-14459.

Verhoeven, K.J.F., & Preite, V. (2014). EPIGENETIC VARIATION IN ASEXUALLY REPRODUCING ORGANISMS. *Evolution*, 68 (3), 644-655.

Vogt, G. (2022). Environmental Adaptation of Genetically Uniform Organisms with the Help of Epigenetic Mechanisms—An Insightful Perspective on Ecoepigenetics. *Epigenomes*, 7 (1), 1.

Voisin, A.S., Suarez Ulloa, V., Stockwell, P., Chatterjee, A., & Silvestre, F. (2022). Genome-wide DNA methylation of the liver reveals delayed effects of early-life exposure to 17-α-ethinylestradiol in the self-fertilizing mangrove rivulus. *Epigenetics*, 17 (5), 473-497.

Wang, Q., Xiong, F., Wu, G., Liu, W., Chen, J., Wang, B., & Chen, Y. (2022). Gene body methylation in cancer: molecular mechanisms and clinical applications. *Clinical Epigenetics*, 14 (1), 154.

West-Eberhard, M.J. (1986). Alternative adaptations, speciation, and phylogeny (A Review). *Proceedings of the National Academy of Sciences*, 83 (5), 1388-1392.

West-Eberhard, M.J., Developmental Plasticity and Evolution. Oxford University Press, 2003.

West-Eberhard, M.J. (2005). Developmental plasticity and the origin of species differences. *Proceedings of the National Academy of Sciences*, 102 (1), 6543-6549.

Yang, X., Han, H., De Carvalho, D.D., Lay, F.D., Jones, P.A., & Liang, G. (2014). Gene Body Methylation Can Alter Gene Expression and Is a Therapeutic Target in Cancer. *Cancer Cell*, 26 (4), 577-590.

Youngson, N.A., & Whitelaw, E. (2008). Transgenerational Epigenetic Effects. *Annual Review of Genomics and Human Genetics*, 9 (1), 233-257.

Zemach, A., McDaniel, I.E., Silva, P., & Zilberman, D. (2010). Genome-Wide Evolutionary Analysis of Eukaryotic DNA Methylation. *Science*, 328 (5980), 916-919.

Zhang, Y.Y., Fischer, M., Colot, V., & Bossdorf, O. (2013). Epigenetic variation creates potential for evolution of plant phenotypic plasticity. *New Phytologist*, 197 (1), 314-322.

Data and code availability

All the data and R scripts from RRBS and pyrosequencing analyses can be found following these GitHub links:

RRBS: https://github.com/gauthieralx/RRBS_gonads

Pyrosequencing: https://github.com/gauthieralx/Master-s-thesis-pyrosequencing

Introduction to scientific research (June 2023)

The introduction to scientific research (bibliographical introduction of the subject submitted in June 2023) is accessible with this link: https://github.com/gauthieralx/Introduction-to-scientific-research

Annexes

1.

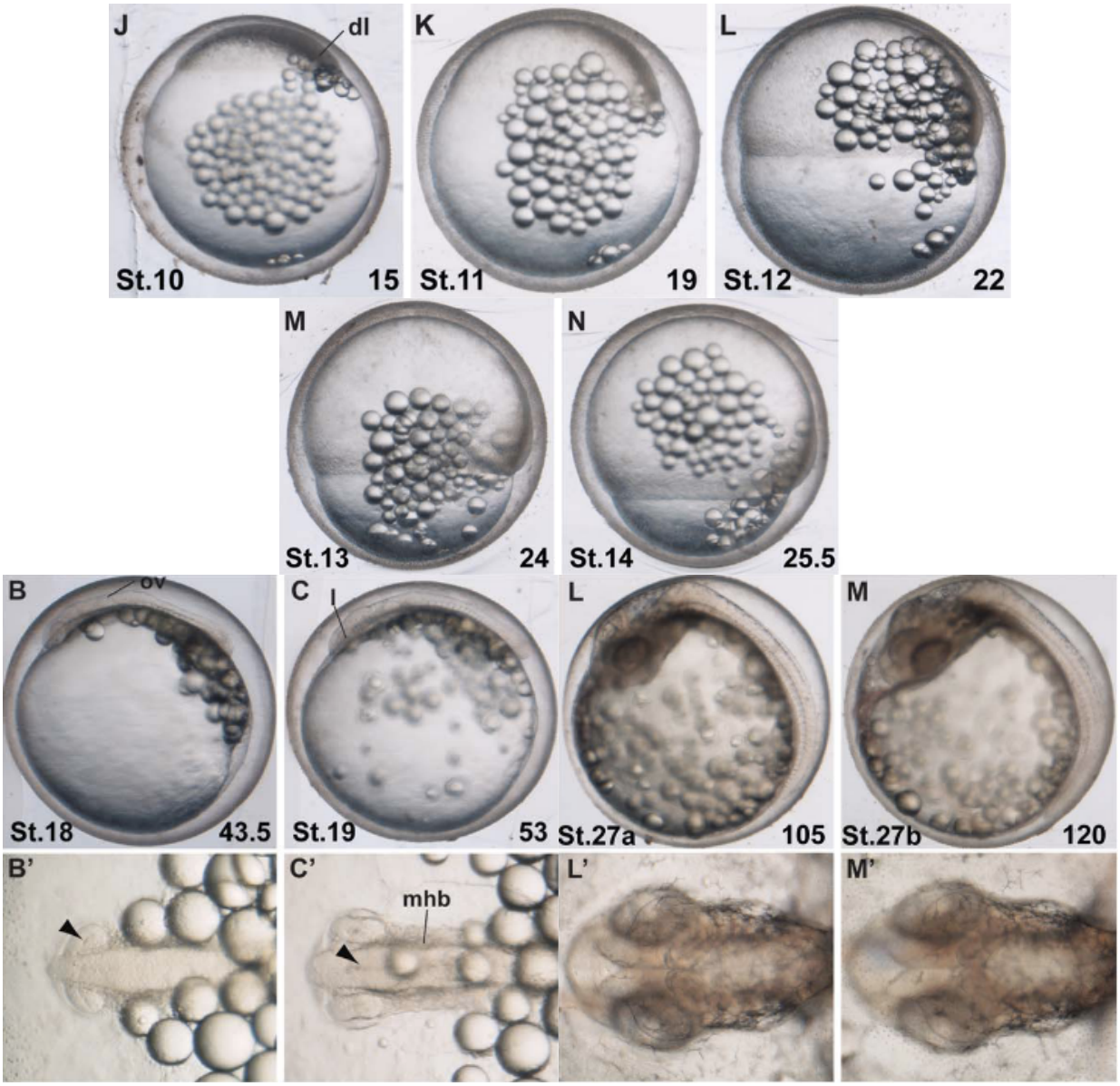

Annex 1: Binocular view of the three embryonic stages studied in the development of *K. marmoratus*. The five upper pictures show the gastrulation stage, namely the beginning of gastrulation (stage (St.) 10), the early gastrula (St. 11), the mid-gastrula (St.

12), the pre-late gastrula (St. 13), and the late gastrula (St. 14). The eight bottom pictures represent the otic vesicle formation (St. 18), the lens formation (St. 19), the increased pigmentation and body movement (St. 27a) and its continuation (St. 27b). All images are lateral views of the embryos, except from St. 18 to St. 27b where the letter's apostrophe shows a head view of the associated stage. Stage numbers are indicated at the bottom left, and time in hours post-fertilization (hpf) is indicated at the bottom right of each picture. dl= dorsal lip, ov= otic vesicle, l= lens, mhb= midbrain-hindbrain boundary. Arrowheads indicate: B'= eye ventricle, C'= brain furrow (from the midbrain to the hindbrain). Scale bars= 200 µm for B', C', L' and M'; 500 µm for all the entire egg views. Pictures are selected from **Mourabit et *al.* (2011)**.

2.

Gene	Gene identity	Forward primer sequence	Reverse primer sequence	Synthesis primer sequence	Target regions
DNMT3a	108233456	TGTGGATTATTTGGTTTATGAGATAATAG	/5Biosg/ACTACTTCTACACCAAATTTATACTCATTA	ATTTGGTTTATGAGATAATAGAT	Promoter
		AGGAAATTTGTTAAGTTTGATTTGTGTG	/5Biosg/AACTAACAACTACCCTAACACAAT	TTTTTATTTTTTTGTTAATAAATAT	Intron 1
		TGATATTTGGAGTGTATATTAGGTAGT	/5Biosg/ACCAAAACTTCAATCTACAACACAT	GGTAGTTAGGTATAAAGTTTTTA	Intron 2
		GGTGGAATTTTGTTGTTATAATGAGA	/5Biosg/TCTCCCAACCACATCACCCA	ATTTTTAGTTTTGTGTTTAATTAGG	Exon 5
MeCP2	108229207	AAAAGGTAGTTGGTTTAAGAAGTTTATATA	/5Biosg/AATTTTATATTAAAAAACTCCAAACATCT	GTTGGTTTAAGAAGTTTATATAT	Promoter
		GGGGAGGTGTGTAGTATAGATGTTTG	CAACCAATTTTACTCAACAAC	AAATTATTTATTTAAATAAAAATGG	Intron 1
		GGGGAGGTGTGTAGTATAGATGTTTG	CAACCAATTTTACTCAACAAC	GGGAATAAGTTATTAATTTAGGG	Exon 3
NIPBL	108234559	/5Biosg/GGGATTAGTTGTAAATTGATGATATAAA	CCCTAAAATTTCTTCTTCTTTTCTTTTAAC	TTTATTTACCTACACAAACTA	Promoter

Annex 2: Table regrouping all the primers and their targeting region previously designed by Chapelle (2023) for gene-specific methylation analysis by pyrosequencing. Various genomic regions are scoped, namely introns, exons and promoter regions. /5Biosg/= 5' Biotin end.

3.

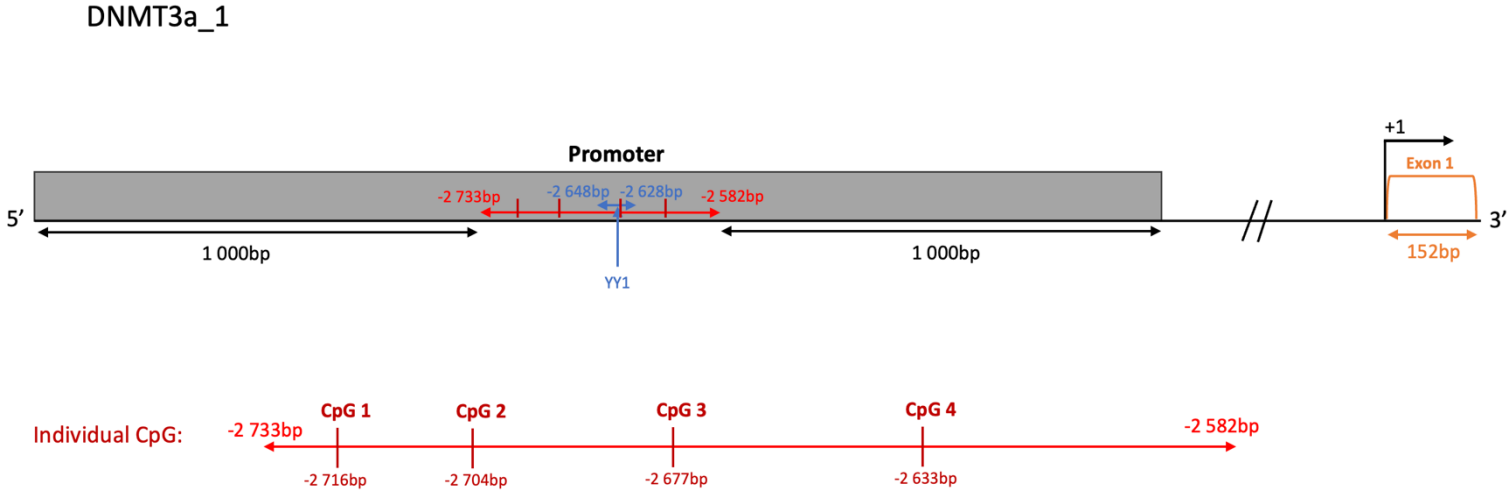

DNMT3a_2

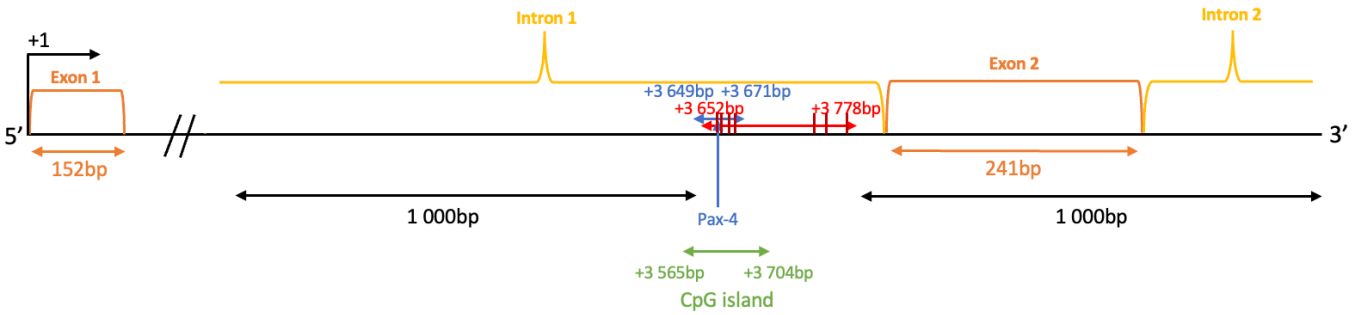

DNMT3a_3

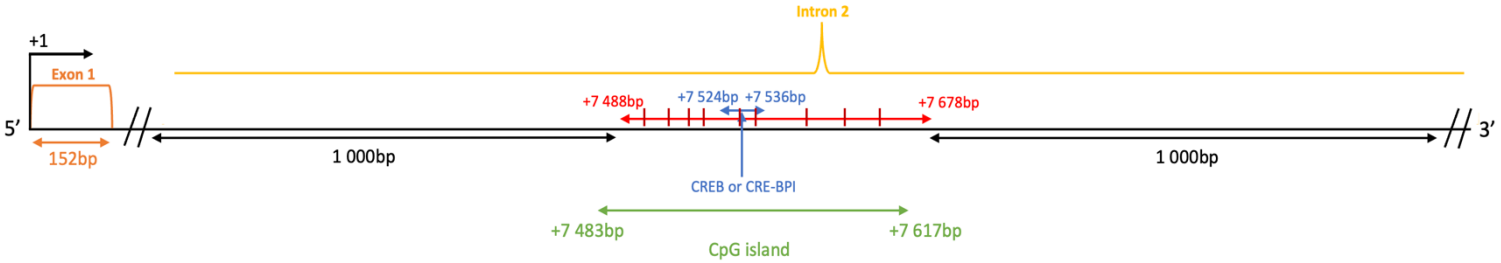

DNMT3a_4

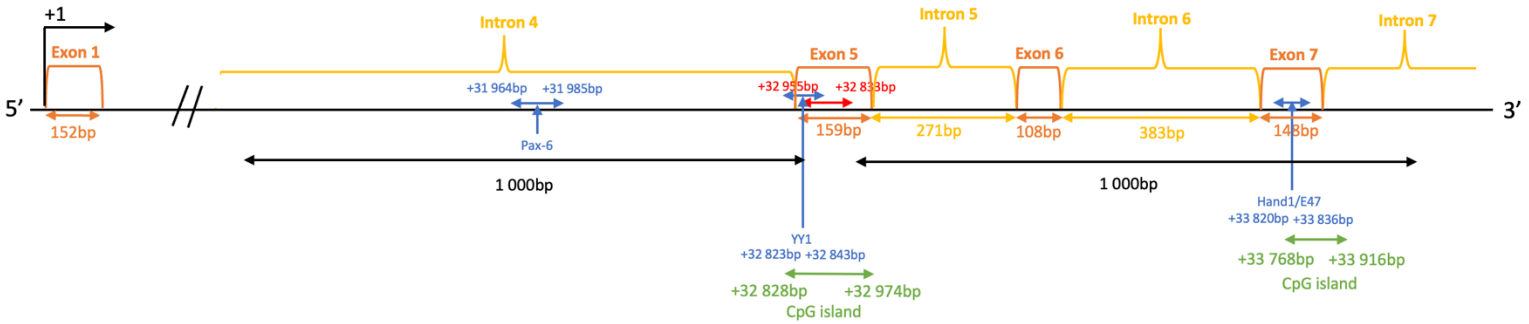

MeCP2_1 & MeCP2_2_2

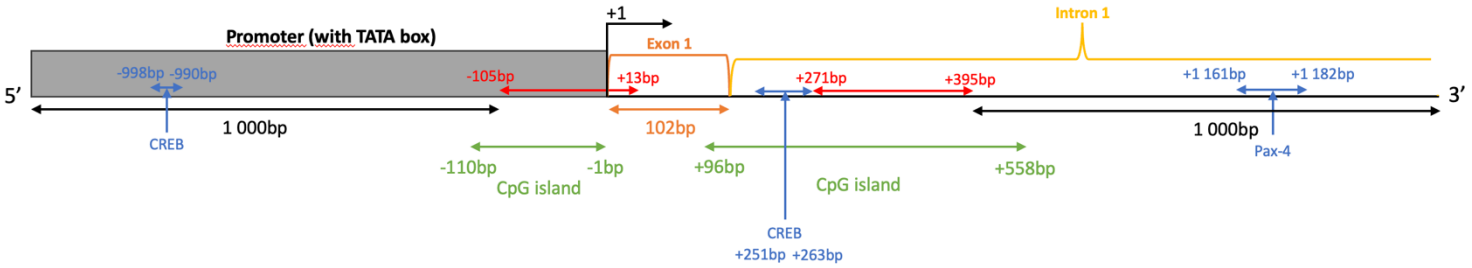

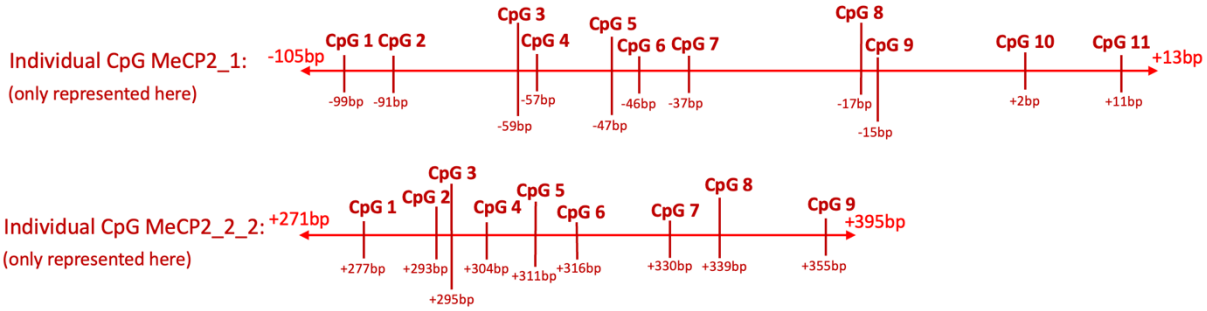

MeCP2_ 3

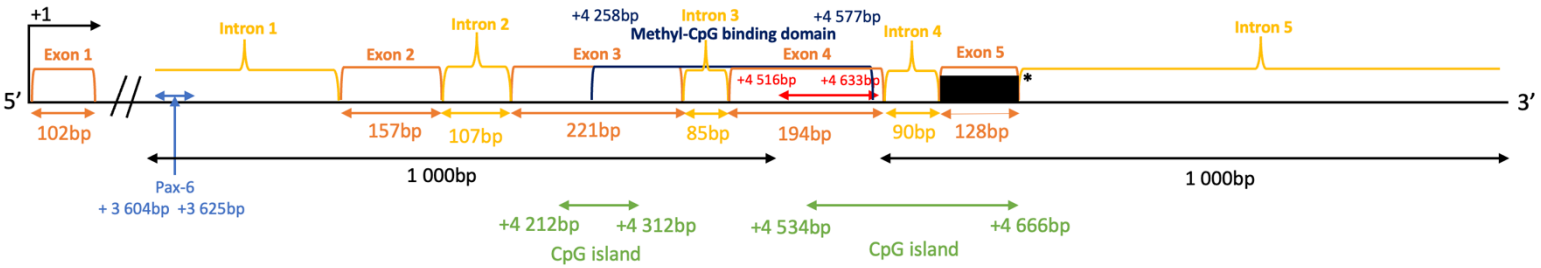

***Transcriptional repression domain**

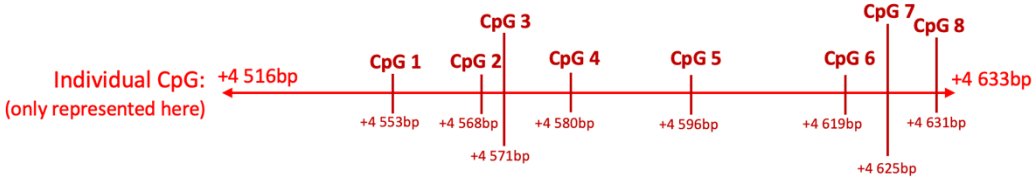

NIPBL

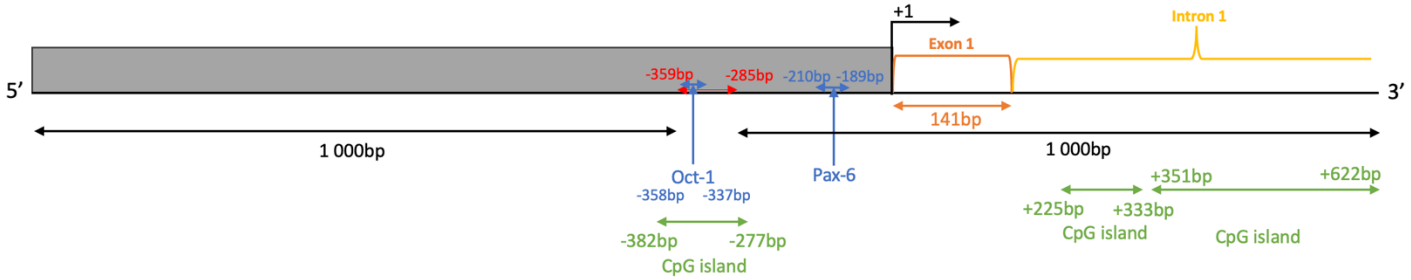

Annex 3: Mapping of the studied sequences from the three genes of interest. From top to bottom: *DNMT3a*: _1= promoter, _2= intron 1, _3= intron 2, _4= exon 5; *MeCP2*: _1= promoter, _2= intron 1, _3= exon 3; *NIPBL*: promoter. The red line represents the studied sequence in the gene, the blue line represents the binding region within the studied sequence of a specific transcriptional factor with its name indicated under the line. The starting site of transcription of the gene is indicated by +1. The numbers indicate the beginning and end of a given sequence in base-pair, related to the +1 starting transcription site. What is found 1 000bp upstream and downstream of the studied sequence is also represented. The name of each genomic region is also indicated. Parallel lines represent a shortcut symbol for shortening the sequence. The precise location of each individual CpG in a sequence is shown in dark red at the bottom of each mapping.

4.

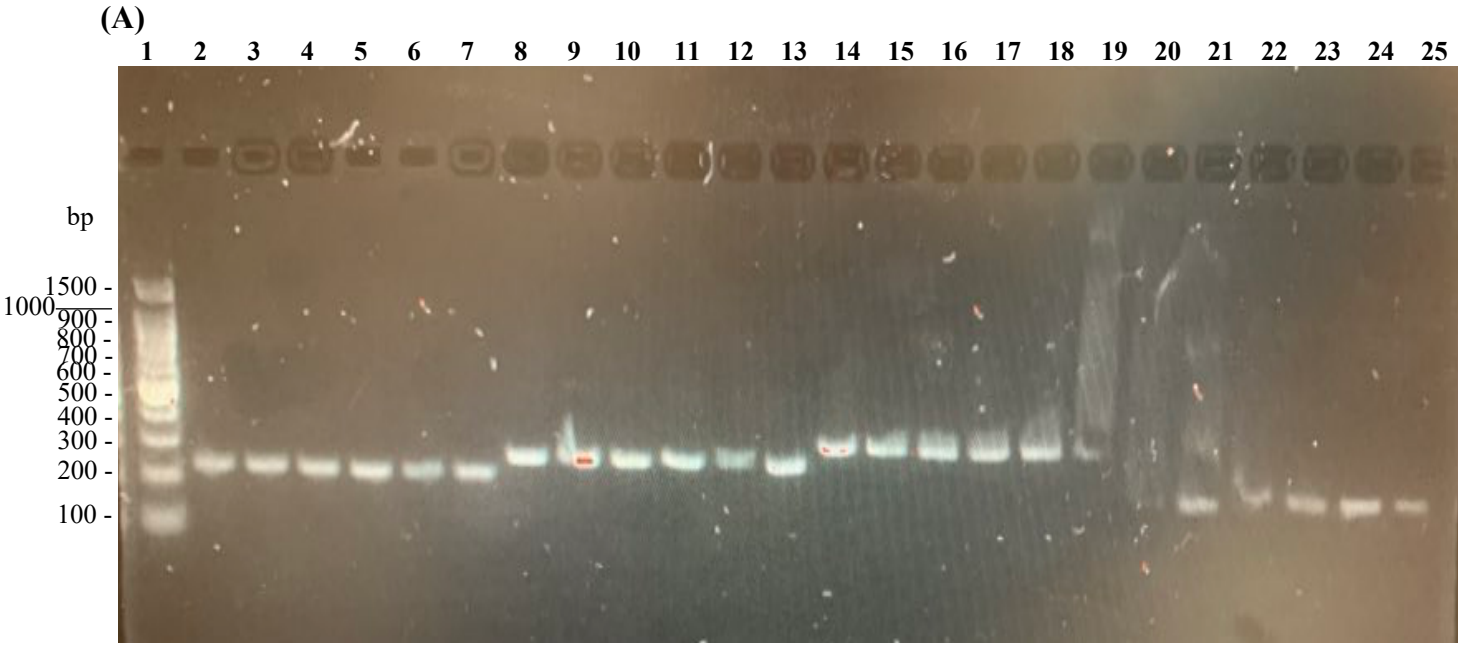

1= BenchTop 100bp DNA Ladder (Promega); *DNMT3a* promoter: **2**= E27:1, **3**= EOL:1, **4**= Egast:1, **5**= T27:1, **6**= TOL:1, **7**= Tgast:1; *DNMT3a* intron 1: **8**= E27:2, **9**= EOL:2, **10**= Egast:2, **11**= T27:2, **12**= TOL:2, **13**= Tgast:2; *DNMT3a* intron 2: **14**= E27:3, **15**= EOL:3, **16**= Egast:3, **17**= T27:3, **18**= TOL:3, **19**= Tgast:3; *DNMT3a* exon 5: **20**= E27:1, **21**= EOL:1, **22**= Egast:1, **23**= T27:1, **24**= TOL:1, **25**= Tgast:1.

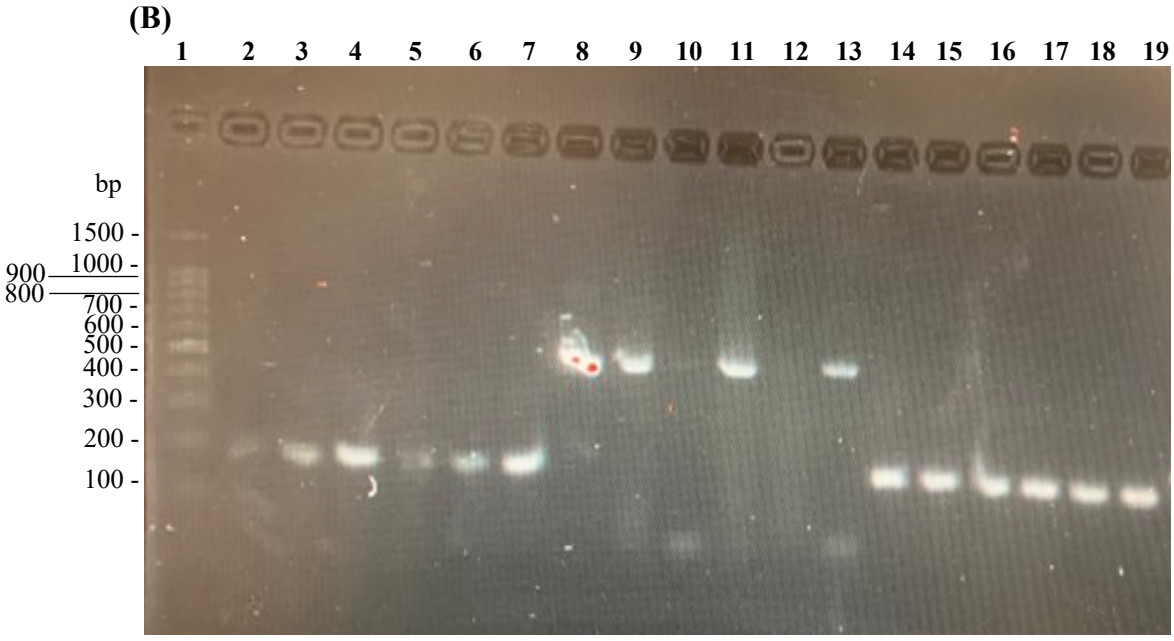

1= BenchTop 100bp DNA Ladder (Promega); *MeCP2* promoter: **2**= E27:1, **3**= EOL:1, **4**= Egast:1, **5**= T27:1, **6**= TOL:1, **7**= Tgast:1; *MeCP2* intron 1: **8**= E27:2, **9**= EOL:2, **10**= Egast:2, **11**= T27:2, **12**= TOL:2, **13**= Tgast:2; *MeCP2* exon 3: **14**= E27:3, **15**= EOL:3, **16**= Egast:3, **17**= T27:3, **18**= TOL:3, **19**= Tgast:3.

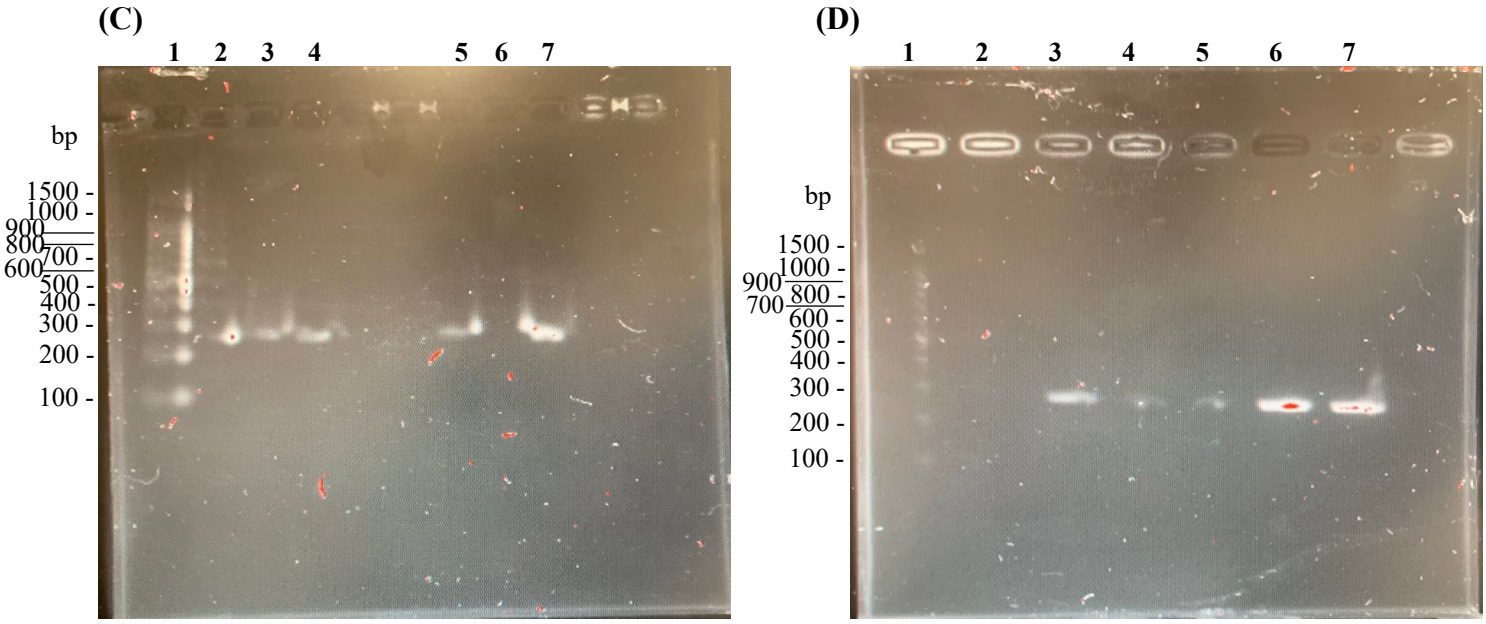

1= BenchTop 100bp DNA Ladder (Promega); *NIPBL* promoter: **2**= E27:1, **3**= EOL:1, **4**= Egast:1, **5**= T27:1, **6**= TOL:1, **7**= Tgast:1.

Annex 4: Gel electrophoreses testing all the sequences of the genes of interest. Each gel was realized with 2% agarose and migrated during 45 minutes under 100V. One of the three replicates for each of the three developmental stages for the two mangrove rivulus populations is tested. Another replicate was tested for a different sequence of the same gene, allowing for the usage of only 2 µL from each replicate of a strip (except for the gastrula and OL stages from TC population for *NIPBL* since they had only one replicate for two gels). (A) Test for 4 *DNMT3a* sequences with 25 wells. (B) Test for 3 *MeCP2* sequences with 19 wells. (C, D) Test for *NIPBL* promoter, with 11 wells for (C) and 8 wells for (D). Two gels were tested for *NIPBL* because of the seemingly low quality of the first gel tried (C), even though the second gel tested (D) doesn't demonstrate much more quality. When comparing both gels at the same time, DNA bands can be discernable for every replicate of the two populations. E= EPP, T= TC; 27 (27^{th} stage), OL (Otic-Lens formation), gast (gastrula stage); :1/2/3= the replicate.

5.

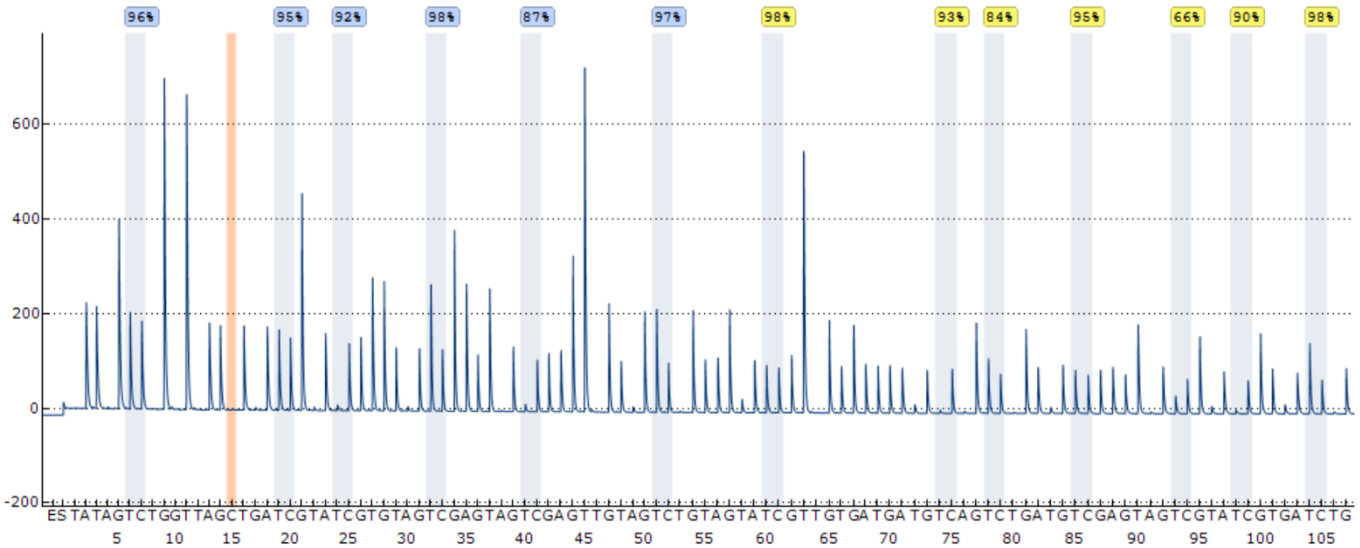

Sequence to analyze:
ATGGTYGGGGTTTTAGTATYGGGAYGTTGGTGTTYGGGAAGTTGYGAGGGTTTTTTTGGTGGTTYGGTAGGATYGTTTTTTGGTGGATGAGYGGTY
GGAGTYGAGTTGYGGAYGGTATTYGT

Annex 5: Example of a pyrogram trace for the 27th stage in the embryonic development of *K. marmoratus* (EPP population), from the exon 5 sequence studied in *DNMT3a*. Y axis represents the relative light units detected when a specific nucleotide is incorporated during sequencing. X axis shows the dispensation order of dNTPs applied throughout sequencing. Each incorporation of dNTP goes along with the release of pyrophosphate (PPi) proportionally to the amount of nucleotide incorporated. PPi permits through a short enzymatic cascade the conversion of luciferin into oxyluciferin by luciferase, generating visible light (seen as a peak in the pyrogram trace). The orange vertical bar represents the bisulfite conversion control (cytosine not in a CpG context), ensuring the correct conversion of unmethylated cytosines into thymines (after PCR) by the bisulfite treatment of DNA. The grey vertical bars indicate the locations of 13 specific CpG sites with the estimated methylation percentage above each position. The color of the methylation percentage indicates the quality of the estimated methylation: blue= passed, yellow= check, red= failed. The bisulfite-treated sequence of DNA to analyze is shown under the pyrogram, where Y indicates a cytosine located in a CpG site.

6.

Sequence	Population	
	EPP	**TC**
DNMT3a_1	Gastrula: 15.8360758 OL: 15.1429564 27th: 14.8555047	Gastrula: 18.3370033 OL: 18.1438520 27th: 16.2696329
DNMT3a_2	Gastrula: 6.5958200 OL: 6.4557356 27th: 5.3487382	Gastrula: 5.6179482 OL: 6.4708177 27th: 5.5913563
DNMT3a_3	Gastrula: 7.1939101 OL: 8.8245585 27th: 6.5231341	Gastrula: 7.2222223 OL: 9.3787438 27th: 4.6622898
DNMT3a_4	Gastrula: 6.6527543 OL: 4.5597372 27th: 6.7227516	Gastrula: 12.4294478 OL: 9.0486598 27th: 8.4503632
MeCP2_1	Gastrula: 1.1259454 OL: 0.9033732 27th: 0.8871889	Gastrula: 0.8517309 OL: 1.3122805 27th: 0.8396612
MeCP2_2_2	Gastrula: 1.1149856	Gastrula: 2.2742094 27th: 1.3585700
MeCP2_3	Gastrula: 16.6636440 OL: 14.0633912 27th: 13.9496861	Gastrula: 15.1606007 OL: 14.5431739 27th: 14.4119339
NIPBL	Gastrula: 0.8774077 OL: 3.7528071 27th: 8.3800343	Gastrula: 0.4178843 OL: 2.3347860 27th: 7.0496913

Annex 6: Table regrouping all the standard deviations for each data point represented in figure 4. The upper and lower boundaries of each data point are calculated by respectively adding or subtracting the standard deviation to the mean value of methylation. OL= Otic-Lens formation, 27th= 27th stage of development.

Supplementary information

1. Change of rivulus and artemia waters

Every Friday, from the beginning of March until the end of December 2023, both the waters of ten chosen fish and of artemias were changed. Ten different fish from a specific population were chosen for the water renewal which consists in throwing the used water into the sink and pouring 500 mL of new 12 ± 1 ppt of saltwater into their tank. Once the renewal was finished, a yellow sticker was added to the fish tank indicating that its water has already been changed. Therefore, every week, ten tanks without a yellow sticker were chosen, following the same population. When the water of all the fish from a specific population was renewed, another population was selected. The water inside artemias' tanks (two tanks) was changed by throwing the used water with the artemias' shells into the sink. The tanks and their associated foam (stopping as much as possible the cysts to come in front of the tank where the living artemias are collected for fish nourishment) were cleaned with a sponge. Finally, new 25 ± 1 ppt of saltwater was poured back in both tanks. Foams and air-pumps in each tank were reset.

Figure S1

Figure S1: Incubators where the fish and the eggs were raised under laboratory conditions. Temperature is set to 25°C, and a photoperiod of 12:12 light:dark is applied. Fish are split following their original population and their age. © Gauthier Alexandrescu.